Cross Sections for Electron Collisions with Water Molecules

Yukikazu Itikawa[a)]
Institute of Space and Astronautical Science, Sagamihara 229-8510 and Department of Physics, Tokyo Metropolitan University, Hachiouji 192-0397, Japan

Nigel Mason
Department of Physics and Astronomy, The Open University, Milton Keynes MK7 6AA, United Kingdom

Received 22 March 2004; revised manuscript received 17 May 2004; accepted 17 June 2004; published online 14 February 2005

Cross section data have been compiled from the literature (to the end of 2003) for electron collisions with water (H_2O) molecules. All major collision processes are reviewed including: total scattering, elastic scattering, momentum transfer, excitation of rotational, vibrational, and electronic states, ionization, electron attachment, dissociation, and emission of radiation. In each case we assess the collected data and provide a recommendation of the values of the cross section to be used. They are presented in a tabular form. Isotope effects (H_2O versus D_2O) are discussed as far as information is available. © *2005 American Institute of Physics.* [DOI: 10.1063/1.1799251]

Key words: attachment; cross section; dissociation; elastic scattering; electron collision; emission; excitation; H_2O; ionization; momentum transfer; recommended data; total scattering; water.

Contents

List of Tables

[a)]Present address: 3-16-3 Miwamidoriyama, Machida 195-0055, Japan; electronic mail: yukitikawa@nifty.com

List of Figures

1. Introduction

Water is the third most abundant molecule in the Universe (after H_2 and CO).[1] Apart from the importance of its maser action, water is expected to contribute significantly to the cooling of star-forming molecular clouds.[2] In the solar system, water vapor has been detected in the atmospheres of Venus, Mars, and the giant planets and even in the solar atmosphere. Water is also the most abundant molecule in comets. In the terrestrial atmosphere, H_2O is the most important greenhouse gas,[3] contributing more than half of the 33 K of natural warming. Water is not a major precursor of global warming but, if the atmosphere warms due to increase in the concentrations of pollutants like CO_2, the atmosphere will be able to hold more water vapor evaporated from surface and hence there will be an amplification of the warming effect. Water is the main product of combustion of hydrocarbon fuels, and hence it is one of the essential ingredients of the model flue gas. Finally water plays an essential role in our life, being the dominant component of the biological cell.

Electron collisions are a fundamental process in all of the phenomena involving water molecules stated above. For example, electron collisions are proposed to play a significant role in determining the rotational population of water molecules in cometary atmospheres.[4] This is of importance in the analysis of the observed emission from the comets. It is now feasible to use plasma techniques to control pollution from fossil fuel combustion. To model such control processes, we need to know the details of the elementary processes in the flue plasma including electron collisions.[5] The initial physical stage of radiation interaction with biological material can be understood on the basis of the analysis of the track structure caused by charged particles. The knowledge of electron interactions with water molecules is therefore vital in understanding radiation damage.[6]

Electron collisions with H_2O have been studied for many years with a large number of papers reporting cross section data for many different interactions. A review of the cross section data has been attempted by several authors. The atomic and molecular data relevant to radiation research were surveyed by a Committee of IAEA. Their report[7] includes cross sections for electron collisions with H_2O. Recently Karwasz *et al.*[8] and Shirai *et al.*[9] have published a data review of electron collisions with molecules, both the reviews including cross section data on H_2O. A recent bibliography prepared by Hayashi[10] may also be useful. Very recently an extensive data compilation has been carried out for electron collisions with a large number of molecules.[11] This work has provided a comprehensive set of cross sections recommended for total scattering, elastic scattering, momentum transfer, ionization, electron attachment, and excitations of vibrational and electronic states. However each of these reviews has some limitations, either in scope or in failing to provide a recommendation of values to be used by the ''applied'' community. The present paper reviews the cross section for electron collisions with H_2O and aims to provide a more complehensive set of data than those published before. The present review is partly based on the Landolt-Börnstein data compilation,[11] but has a wider scope (e.g., including emission cross sections). After reviewing avaliable cross section data, we have determined a set of recommended values of cross section, when possible. The quality of the recommended data is not uniform over the processes considered. This reflects the situation that the availability of reliable data

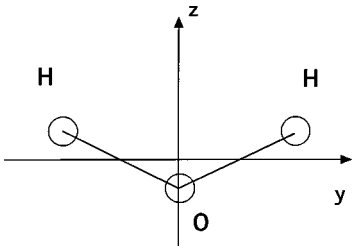

FIG. 1. Nuclear configuration of H_2O.

is different depending on the process. The general criteria for the selection of preferred data are as follows:

(1) In principle, experimental data are preferred to theoretical ones. In some cases, however, elaborate calculations are referred to corroborate the experimenal work.

(2) The reliability of the experimental methods empolyed is critically assessed. Agreement between multiple independent measurements of the same cross section is generally taken as an endorsement of the accuracy of the measured data. A strong emphasis is placed on the consistency of the results taken by completely different techniques.

(3) In cases where only a single set of data is available for a given cross section, those data are simply shown here (i.e., not designated as recommended), unless there is a strong reason to reject them.

More details of the process of data evaluation can be found in each section.

To make a discussion more complete, information about the electron collisions with D_2O (i.e., an isotope effect) is also presented. To the knowledge of the present authors, no information is available on the electron collisions with T_2O.

The literature has been surveyed through the end of 2003.

2. The Molecular Properties of H_2O

Water molecule in its electronically ground state has a C_{2v} symmetry (see Fig. 1). The equilibrium nuclear configuration has[12]

$$r_{OH}=0.095\,792 \text{ nm},$$

$$\theta(\text{H–O–H})=104.5°.$$

The ionization energy of H_2O recommended by Lias[13] is

$$E_i=12.621(\pm 0.002) \text{ eV}.$$

After a very extensive critical assessment of the available data, Ruscic *et al.*[14] determined the best value of the dissociation energy to be

$$D(\text{H–OH})=5.0992(\pm 0.0030) \text{ eV}.$$

Here both the dissociation products are in their electronically ground states. Other dissociation channels are listed in Sec. 10.

H_2O has a permanent electric dipole moment. Its direction is along the symmetry axis of the molecule (i.e., the z axis in Fig. 1), and its magnitude is[15]

TABLE 1. Vibrational levels of H_2O

v[a]	Energy[b] (eV)
010	0.1977
020	0.3907
100	0.4534
001	0.4657
030	0.5786
110	0.6491
011	0.6610
040	0.7605
120	0.8400
021	0.8520
200	0.8929
101	0.8989
002	0.9231

[a]Vibrational states are denoted by the quantum number $v=(v_1,v_2,v_3)$, where v_1,v_2,v_3 represent the symmetric-stretching, bending, and antisymmetric stretching states, respectively.
[b]Summarized by Polyansky *et al.*[20]

$$\mu_z=1.8546 \text{ D}=0.729\,65 \text{ a.u.}$$

This was determined by the spectroscopic measurement of the Stark effect in the rotational spectrum.[16] The electric quadrupole moment of H_2O has three components:[17]

$$\Theta_{xx}=-2.50\times 10^{-26} \text{ esu cm}^2,$$

$$\Theta_{yy}=2.63\times 10^{-26} \text{ esu cm}^2,$$

$$\Theta_{zz}=-0.130\times 10^{-26} \text{ esu cm}^2.$$

These values were obtained by a high-resolution study of the Zeeman effect in the rotational spectrum. The dipole polarizability also has three components[18]

$$\alpha_{xx}=1.41\times 10^{-24} \text{ cm}^3,$$

$$\alpha_{yy}=1.53\times 10^{-24} \text{ cm}^3,$$

$$\alpha_{zz}=1.47\times 10^{-24} \text{ cm}^3.$$

The mean polarizability is

$$\alpha_0=1.47\times 10^{-24} \text{ cm}^3.$$

H_2O has three normal modes of vibration. Their fundamental frequencies are:[19]

$$\nu_1(\text{symmetric stretching})=3657 \text{ cm}^{-1},$$

$$\nu_2(\text{bending})=1595 \text{ cm}^{-1},$$

TABLE 2. Measurements of total scattering cross section for H_2O

Author(s)	Energy range (eV)
Szmytkowski[21]	0.5–80
Zecca *et al.*[22]	81–3000
Nishimura and Yano[23]	7–500
Saglam and Aktekin[24]	25–300
Saglam and Aktekin[25]	4–20
Kimura *et al.*[26a]	1–400

[a]A revision of measurement by Sueoka *et al.*[27]

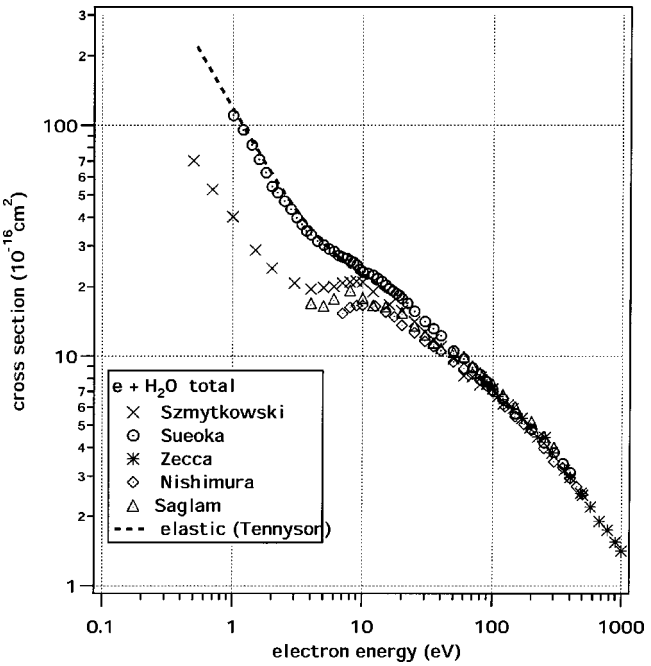

FIG. 2. Total scattering cross section, Q_T, of H_2O. A comparison is made of the experimental cross sections obtained by Szmytkowski (Ref. 21), Sueoka *et al.* (Ref. 26), Zecca *et al.* (Ref. 22), Nishimura and Yano (Ref. 23), and Saglam and Aktekin (Refs. 24 and 25). The theoretical elastic cross section obtained by Tennyson *et al.* (Ref. 28) is also shown for comparison.

$$\nu_3(\text{antisymmetric stretching}) = 3756 \text{ cm}^{-1}.$$

Observed energies of the vibrational levels were summarized by Polyansky *et al.*[20] The lowest 13 levels (i.e., those below the second harmonic of antisymmetric stretching mode) are shown in Table 1.

The rotational motion of water molecule is described by that of an asymmetric-top rotor. The rotational energy levels are presented in Sec. 5.

Electronically excited states are discussed in Sec. 7.

3. Total Scattering Cross Sections

The total scattering cross section (Q_T) of H_2O has been measured by several groups.[21–26] Table 2 lists these measurements and the energy range over which they were recorded. Figure 2 compares these results. The Q_T of the different groups are in good agreement at the energies above about 30 eV. However in the lower energy region, they differ significantly from one another. At 10 eV, for example, the values of Q_T measured by Nishimura and Yano,[23] Saglam and Aktekin,[25] Szmytkowski,[21] and Kimura *et al.*[26] are 16.6, 17.8, 20.9, and 23.2 in units of 10^{-16} cm^2, respectively. Hence the relative difference amounts to about 40%. These disagreements may be attributed to the uncertainty of each experiment in determining contributions to Q_T from forward scattering. In electron collisions with H_2O, the elastic (or more precisely, vibrationally elastic) cross section is very sharply peaked in the forward scattering direction (see Sec. 4). This is due to the strong dipole moment of the molecule. Thus forward scattering is a large fraction of Q_T.

All the measurements listed in Table 2 are based on the electron transmission method. Usually in the method, the detector cannot totally discriminate against electrons elastically scattered at the angles smaller than a certain value (denoted by θ_{min} here) which is determined by the acceptance angle of the apparatus. In other words, we have the relation

$$Q_T = Q_T(\text{measured}) + \Delta Q_T. \tag{1}$$

Here Q_T(measured) is the measured value of Q_T and is defined by

$$Q_T(\text{measured}) = 2\pi \int_{\theta_{min}}^{\pi} q(\theta) \sin\theta \, d\theta, \tag{2}$$

where $q(\theta)$ is the differential cross section. Furthermore in the actual experiment, θ_{min} depends on the scattering center in the collision chamber, and hence it is not easy to estimate the correction, ΔQ_T, precisely. All the authors of the above papers recognized this problem and tried to estimate the uncertainty arising from the necessary correction to their recorded data. For example, Szmytkowski[21] stated that the contribution of the forward scattering was about 0.4% of the measured Q_T at energies of 2 eV and below. Sueoka and his colleagues refined their earlier data to allow for θ_{min} and revised their earlier measurement.[27] The revised Q_T is reported in their review paper.[26]

In the energy region below about 10 eV, we have the relation

$$Q_T = Q_{elas}. \tag{3}$$

Here Q_{elas} is the vibrationally elastic cross section (for the magnitude of inelastic cross sections, see later sections). Recently Tennyson and his colleagues[28] have made an elaborate calculation of Q_{elas} (for details, see Sec. 4). Figure 2 shows also their elastic cross section. The Q_T of Kimura *et al.*[26] is in very good agreement with this theoretical Q_{elas} and supports the reliability of the Q_T of Kimura *et al.*[26] A detailed comparison shows that the Q_T of Kimura *et al.* is somewhat smaller than the Q_{elas} at the energies below 5 eV. (At 2 eV, for example, the Q_T is smaller than the Q_{elas} by about 14%.) This discrepancy may be within the uncertainty of these measured cross sections. However Kimura *et al.* did not state error bars for all their results in H_2O, but in their measurement of a similar polar molecule, HCl,[29] they claimed an error of 13% at 1 eV. In their calculations of Q_{elas}, Tennyson *et al.* assumed that the water molecule is initially in its rotationally ground state. Okamoto *et al.*[30] showed in their calculation of elastic cross section that, if one considers the distribution of rotational states at room temperature, the resulting value of Q_{elas} is decreased by about 10% at 6 eV. Considering these two points (i.e., uncertainty of the experiment and the rotational distribution in theory), the agreement between the theoretical Q_{elas} and the Q_T of Kimura *et al.* would become much better than shown in the figure. Therefore for low energies (<10 eV) we recommend the values of Kimura *et al.* with an error of 15%.

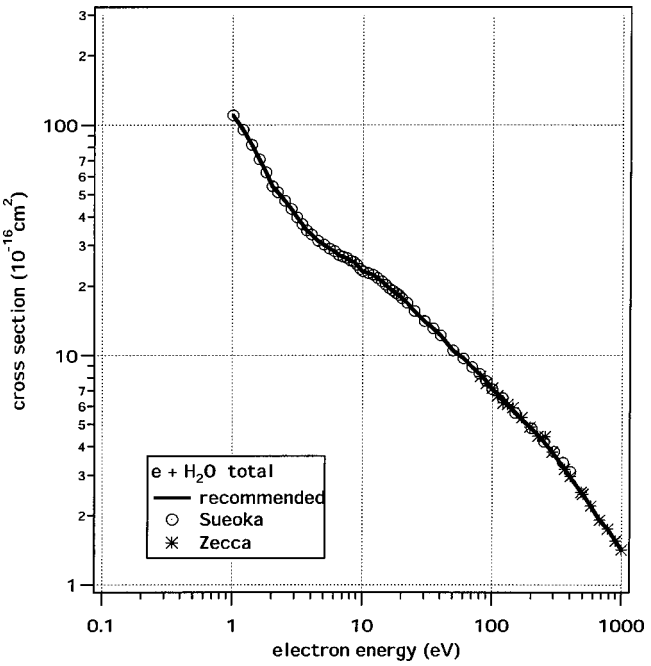

FIG. 3. Recommended values of Q_T for H_2O, compared with the experimental values obtained by Sueoka *et al.* (Ref. 26) and Zecca *et al.* (Ref. 22).

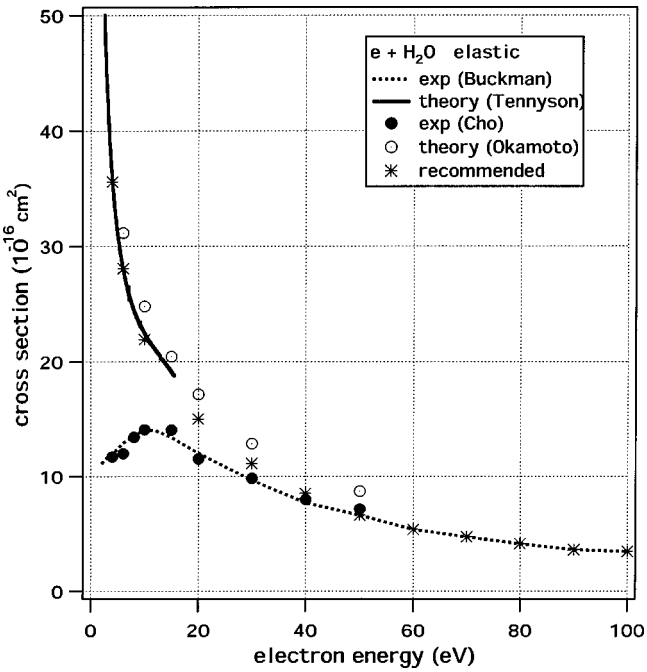

FIG. 4. Elastic scattering cross sections, Q_{elas}, of H_2O. The present recommended values are compared with those recommended by Buckman *et al.* (Ref. 37), experimental data obtained by Cho *et al.* (Ref. 38), and theoretical values obtained by Tennyson *et al.* (Ref. 28) and Okamoto *et al.* (Ref. 30).

Kimura *et al.* reported their Q_T up to 400 eV. In the energy range above that, only Zecca *et al.*[22] have reported an extensive measurement. The Q_T of Zecca *et al.* are consistent with the Q_T of Kimura *et al.* in the region where the two sets of measurements overlap. Thus we have smoothly connected the two sets of cross sections to produce the recommended data on Q_T over the energy range, 1–1000 eV (Fig. 3). Table 3 gives the numerical values of the recommended Q_T.

TABLE 3. Recommended total scattering cross section for electron collisions with H_2O

Energy (eV)	Cross section (10^{-16} cm^2)	Energy (eV)	Cross section (10^{-16} cm^2)	Energy (eV)	Cross section (10^{-16} cm^2)
1	110	8	25.8	50	10.5
1.2	95.3	8.5	25.5	60	9.7
1.4	82.0	9	24.8	70	8.9
1.6	71.0	9.5	23.7	80	8.3
1.8	62.3	10	23.2	90	7.7
2	54.2	11	22.8	100	7.1
2.2	51.1	12	22.4	120	6.5
2.5	46.9	13	21.7	150	5.6
2.8	43.2	14	21.0	200	4.8
3.1	39.8	15	20.3	250	4.2
3.4	37.2	16	19.6	289	3.78
3.7	34.8	17	19.1	361	3.19
4	33.5	18	18.6	400	2.93
4.5	31.4	19	18.3	484	2.53
5	30.2	20	17.7	500	2.48
5.5	29.1	22	16.9	576	2.20
6	28.4	25	15.6	676	1.91
6.5	27.3	30	14.1	782	1.75
7	26.8	35	13.1	900	1.55
7.5	26.5	40	12.2	1000	1.42

The total scattering cross section for D_2O has been measured by Nishimura and Yano[23] and Szmytkowski *et al.*[31] Their values of Q_T are in agreement with the corresponding values for H_2O within the combined experimental errors. Szmytkowski *et al.* claimed, however, that the small difference was real and mainly due to rotational and vibrational excitations of the respective molecules. However considering the uncertainty of the Q_T in the lower energy region discussed above, no definitive conclusions about the magnitude of the isotope effect on Q_T can be made.

4. Elastic Scattering and Momentum-Transfer Cross Sections

Almost all the electron beam experiments have insufficient energy resolution to resolve each rotational state of the water molecule. Hence any elastic cross section, Q_{elas}, obtained experimentally is only vibrationally elastic: i.e., including the cross section for rotational transitions, averaged over the initial rotational states and summed over the final ones. In the present section, therefore, Q_{elas} is defined as the vibrationally elastic cross section. Pure elastic, or rotationally elastic, cross sections are discussed in Sec. 5.

After surveying the available experimental results,[32–36] Buckman *et al.*[37] recently presented their recommended values of Q_{elas}. They claimed 40% accuracy in the resulting data. Until recently beam experiments were unabale to measure differential cross section (DCS) in the forward or in the backward scattering directions. To derive integral cross section (ICS), the measured DCS were extrapolated towards 0°

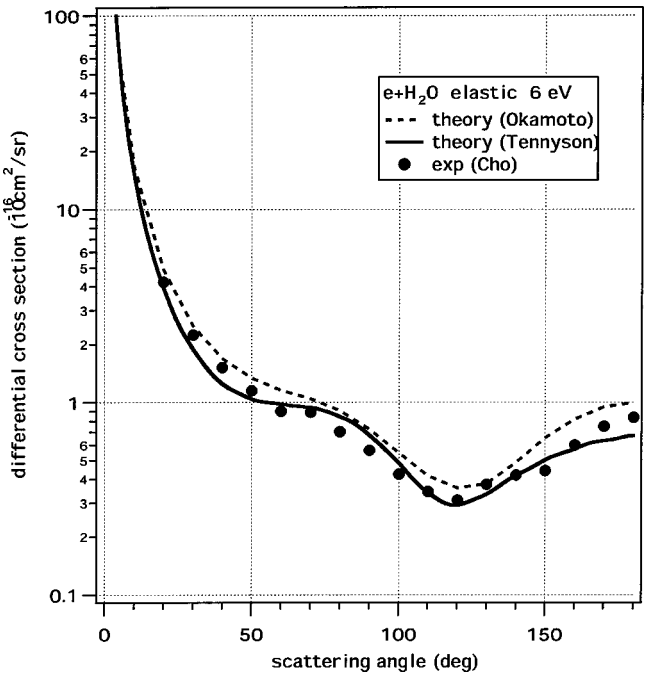

FIG. 5. Differential cross sections for the elastic scattering from H_2O at the collision energy of 6 eV. Theoretical values obtained by Tennyson *et al.* (Ref. 39) and Okamoto *et al.* (Ref. 30) are compared with experimental data of Cho *et al.* (Ref. 38).

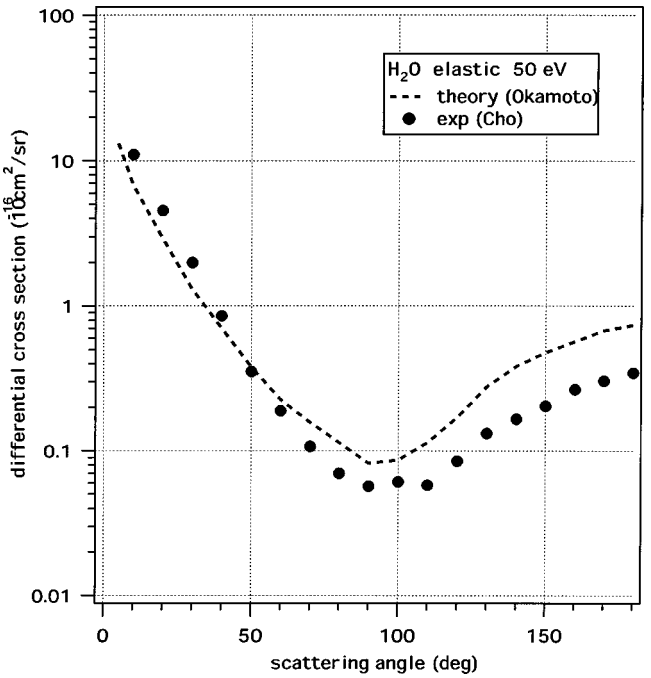

FIG. 6. Differential cross sections for the elastic scattering from H_2O at the collision energy of 50 eV. Theoretical values obtained by Okamoto *et al.* (Ref. 30) are compared with experimental data of Cho *et al.* (Ref. 38).

and 180°. This results in an uncertainty in the derived ICS. Very recently, Cho *et al.*[38] succeeded in measuring the DCS at 10°–180°, with the use of a magnetic-angle-changing device. In Fig. 4, the ICS they determined are compared with the values recommended by Buckman *et al.* There is a good agreement between the two sets of Q_{elas}.

As is described in the previous section, Tennyson and his colleagues[28] obtained Q_{elas} using the R-matrix theory. In Fig. 4, their theoretical result is compared with another theoretical one by Okamoto *et al.*[30] and the experimental data of Cho *et al.* There is a large disagreement between the theoretical and the experimental values at energies below 20 eV, but the discrepancy decreases with increasing energy. Figure 5 shows a corresponding comparison of DCS at 6 eV. The theoretical DCSs (particularly those of Tennyson *et al.*, which are shown in the paper by Faure *et al.*[39]) agree very well with the experimental DCS of Cho *et al.* This indicates that the difference in the ICSs shown in Fig. 4 is ascribed to the difference in the contribution of the DCS at the angles smaller than 20°. Cho *et al.* estimated the contribution by a multiparameter fitting of the measured DCS. Because of the strong dipole moment of the molecule, the elastic DCS for H_2O has a very sharp peak in the forward direction (according to the theory,[28] the DCS at 2° has a value of 3.71×10^{-14} cm^2 at 6 eV). It is therefore likely that any extrapolation procedure will introduce a large systematic error. For example use of a polynomial fit may result in an underestimate of the cross section at $\theta \approx 0°$. On the other hand, theory can reliably take into account the dipole effect, which dominates at the lower collision energy. Furthermore, as shown in Sec. 3, the theoretical elastic cross section agrees well with the recommended values of the total cross section in the energy range below about 10 eV. As a result, we recommend the theoretical cross sections of Tennyson *et al.*[28] for use at 6 eV and below.

Figure 6 shows a similar comparison of DCS at 50 eV. At this energy, only the theoretical cross section of Okamoto *et al.* is available for comparison with experiment. From this figure, we can conclude that the theoretical ICS is too large compared with experiment at 50 eV. Hence we prefer to recommend the experimental data at 50 eV and above. To provide the recommended cross section in the energy region 6–50 eV, we simply interpolate the two sets of cross sec-

TABLE 4. Recommended elastic scattering cross sections for $e + H_2O$

Energy (eV)	Cross section (10^{-16} cm^2)
1	117
2	61.8
4	35.6
6	28.1
10	21.9
20	15.0
30	11.1
40	8.5
50	6.62
60	5.37
70	4.72
80	4.13
90	3.60
100	3.43

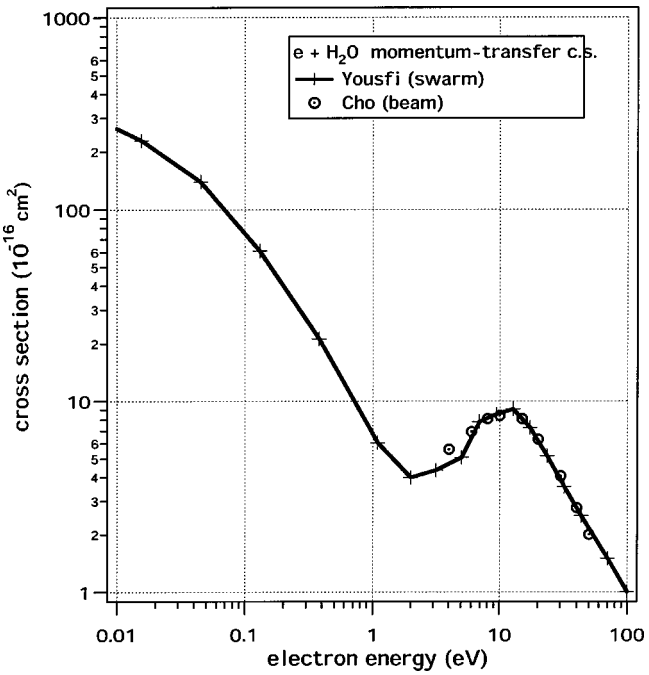

FIG. 7. Momentum transfer cross sections, Q_m, of H_2O. Swarm data (Yousfi and Benabdessadok, Ref. 40) are compared with beam data [Cho *et al.* (Ref. 38)].

tions: the theoretical ones below 6 eV and the experimental ones above 50 eV. The resulting recommended values of Q_{elas} are shown in Fig. 4 with crosses. The numerical values of Q_{elas} thus recommended are given in Table 4. We would however recommend that new experimental data be collected (using the magnetic-angle-changing technique) for energies below 10 eV and that more elaborate theoretical calculations be performed above 20 eV.

TABLE 5. Recommended momentum transfer cross sections for $e+H_2O$

Energy (eV)	Cross section (10^{-16} cm^2)
0.001 861	430.3
0.005 393	325.0
0.015 63	228.4
0.045 28	139.2
0.1312	60.71
0.3802	21.11
1.102	6.042
1.989	3.975
3.16	4.334
5.02	5.055
6.909	7.769
9.386	8.529
12.75	9.052
17.32	7.244
23.53	5.15
31.96	3.561
43.42	2.5
70	1.5
100	1

TABLE 6. Rotational energy levels of H_2O

Para			Ortho		
$J_{K'K''}$	J_τ	Energy[a] (meV)	$J_{K'K''}$	J_τ	Energy[a] (meV)
0_{00}	0_0	0.0	1_{01}	1_{-1}	2.950
1_{11}	1_0	4.604	1_{10}	1_1	5.253
2_{02}	2_{-2}	8.690	2_{12}	2_{-1}	9.856
2_{11}	2_0	11.800	2_{21}	2_1	16.726
2_{20}	2_2	16.882	3_{03}	3_{-3}	16.956
3_{13}	3_{-2}	17.640	3_{12}	3_{-1}	21.495
3_{22}	3_0	25.578	3_{21}	3_1	26.304
3_{31}	3_2	35.363	3_{30}	3_3	35.387

[a]Summarized by Tennyson *et al.*[41]

The momentum-transfer cross section is defined by the formula

$$Q_m = 2\pi \int_0^\pi (1-\cos\theta) q_{elas}(\theta) \sin\theta \, d\theta, \tag{4}$$

where q_{elas} is the elastic differential cross section.

Momentum-transfer cross sections, particularly those at low energies, may be determined by swarm experiments. The most recent swarm measurement is that performed by Yousfi and Benabdessadok[40] and plotted in Fig. 7. According to its definition, Q_m is also obtained from the DCS for elastic scattering measured by beam experiments. By definition, a large-angle scattering contributes to Q_m much more than a small-angle one. Because Cho *et al.*[38] measured DCS up to 180°, their Q_m is expected to be most accurate. (Note that, since the forward scattering has a less significant contribution to Q_m, the extrapolation in the forward direction should have a small effect in this case.) Their derived Q_m are also plotted in Fig. 7. The figure clearly shows that the swarm data are almost in agreement with the beam data of Cho *et al.* In conclusion, the swarm values of Q_m are recommended and are tabulated in Table 5.

5. Rotational Transitions

Rotational motion of water molecule is represented by that of an asymmetric-top rotor. Its energy levels are labeled by a quantum number $J_{K'K''}$, where J is the rotational angular momentum, K' is the projection of J along the axis of least moment of inertia (i.e., the y axis in Fig. 1), and K'' is the projection along the largest moment of inertia (the x axis). Instead of using (K',K''), the levels are often denoted by a pseudoquantum number τ, which is defined by

$$\tau = K' - K''. \tag{5}$$

The rotational energy levels of water are separated into two sets, the one with even values of τ (para levels) and the other with odd values of τ (ortho levels). Neither photoabsorption nor electron impact can induce a transition between the two sets of rotational states. Experimental values of the rotational energy levels of H_2O have been summarized by Tennyson *et al.*[41] Table 6 shows them with $J=0-3$.

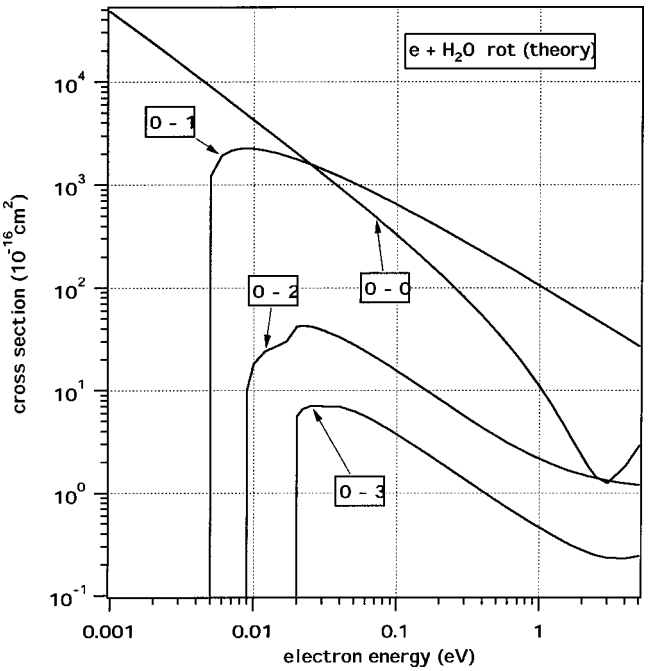

FIG. 8. Cross sections for the rotational transitions, $J=0-0,1,2,3$, of H_2O, calculated by Tennyson *et al.* (Ref. 39).

Tennyson and his colleagues[39,42] have made a comprehensive calculation of the cross section for electron-impact rotational transitions of H_2O using the R-matrix method. Their calculation was based on the fixed-nuclei approximation, corrected with the Born-closure formula for the dipole allowed transition and with a simple kinematic ratio for the threshold behavior. They obtained cross sections for the transitions among all the rotational levels up to $J=5$ at the collision energies 0.001–7.0 eV. Representative values shown in Fig. 8 (and Table 7 and Table 8) present the cross sections for the transitions from the rotationally ground state $J_\tau=0_0$. For simplicity of presentation, they are the cross sections summed over τ, i.e.,

$$Q_{\rm rot}(0\rightarrow J)=\sum_{\tau} Q_{\rm rot}(0_0\rightarrow J_\tau). \tag{6}$$

According to the selection rule, only the para states can be excited from $J_\tau=0_0$.

The calculation shows that:

(i) Among the inelastic processes, the dipole-allowed transition dominates over others. In the transition from $J=0$, $Q_{\rm rot}(0\rightarrow 1)$ is a factor of 40–50 larger than $Q_{\rm rot}(0-2)$, which is the largest of the dipole forbidden processes.

(ii) At around 1 eV, the rotationally elastic (i.e., $J=0\rightarrow 0$) cross section is much smaller than $Q_{\rm rot}(0\rightarrow 1)$. It increases, however, with decreasing energy and exceeds $Q_{\rm rot}(0\rightarrow 1)$ at $E=0.025$ eV and below.

It should be noted, however, that the fixed-nuclei approximation may fail at lower energies. According to the authors of the calculation, the data shown here at the energies below 0.1 eV should be used with caution.

In the higher energy region (6–50 eV), Gianturco *et al.*[43] reported another calculation. They reported cross sections only for the transition from the rotationally ground state ($J=0$). A comparison at 6 eV shows that, for the dominant processes (i.e., $J=0\rightarrow J=0,1$), the two sets of cross sections

TABLE 7. Recommended cross sections (in 10^{-16} cm^2) for electron-impact rotational transitions of H_2O.[39]

Energy (eV)	$J=0-1$	$J=0-2$	$J=0-3$	$J=0-0$
0.001				48 153
0.002				23 600
0.003				15 411
0.004				11 358
0.005	1214			8952
0.006	1915			7365
0.007	2152			6241
0.008	2236			5405
0.009	2252	10.18		4760
0.01	2233	18.16		4248
0.012	2151	24.10		3486
0.015	1998	27.53		2735
0.017	1898	30.12		2385
0.02	1761	41.91	5.580	1997
0.022	1679	42.71	6.584	1798
0.025	1570	41.87	7.069	1562
0.03	1417	38.88	7.011	1277
0.04	1191	32.65	6.909	926.3
0.05	1033	27.74	6.288	720.4
0.06	914.5	24.02	5.595	585.4
0.07	823.0	21.14	4.997	490.3
0.08	749.8	18.86	4.498	420.0
0.09	689.7	17.01	4.083	365.8
0.1	639.5	15.49	3.734	323.0

TABLE 8. Recommended cross sections (in 10^{-16} cm^2) for electron-impact rotational transitions of H_2O.[39] (Continued)

Energy (eV)	$J=0-1$	$J=0-2$	$J=0-3$	$J=0-0$
0.12	560.0	13.14	3.183	259.6
0.15	474.5	10.70	2.603	197.5
0.17	431.8	9.526	2.320	168.9
0.2	381.6	8.184	1.995	137.3
0.22	354.6	7.486	1.824	121.2
0.25	321.2	6.644	1.618	102.3
0.3	278.6	5.613	1.362	79.74
0.4	221.8	4.334	1.040	52.71
0.5	185.4	3.582	0.8458	37.42
0.6	159.9	3.092	0.7168	27.81
0.7	140.9	2.750	0.6251	21.34
0.8	126.2	2.498	0.5566	16.77
0.9	114.5	2.305	0.5036	13.42
1	104.9	2.153	0.4613	10.90
1.2	90.04	1.929	0.3983	7.452
1.5	74.63	1.712	0.3362	4.507
1.7	67.15	1.614	0.3079	3.345
2	58.54	1.509	0.2775	2.262
2.2	54.02	1.458	0.2631	1.821
2.5	48.50	1.398	0.2475	1.432
3	41.60	1.326	0.2331	1.252
4	32.63	1.239	0.2287	1.828
5	27.02	1.204	0.2431	2.884

agree with each other, but there is a somewhat large disagreement for other processes. Combining the results of the two calculations, we can say that, in the energy range 0.1–10 eV, the dipole-allowed rotational transition has the dominant contribution to the vibrationally elastic cross section (i.e., Q_{elas} in Sec. 4) and otherwise the rotationally elastic process (i.e., $J=0-0$) also has a sizable contribution to Q_{elas}.

The only experimental attempt to investigate rotational transitions was made by Jung *et al.*[44] They could not resolve each rotational transition but obtained the excitation and deexcitation cross section as a sum, respectively. Furthermore they reported only DCS at 2.14 and 6.0 eV. Gianturco *et al.* compared their calculation with the measured DCS and found a qualitatively good agreement. However, given the improvement in stability and resolution of modern electron spectrometers, it would be timely to remeasure the values of Jung *et al.*

Due to the small interlevel spacings, water molecules in the gas phase at a finite temperature will be populated over a large range of rotational states. At 300 K, for example, the states with $J=1-5$ have a significant population. In making allowance for such states in electron scattering, we believe that the paper of Faure *et al.*[39] should be referred to for the transitions from those states.

Faure *et al.*[39] also calculated the rotational cross section for D_2O. Their calculation shows that the $Q_{\mathrm{rot}}(0\rightarrow1)$ for D_2O is always larger than that for H_2O. For example, the ratio $Q_{\mathrm{rot}}(0\rightarrow1,D_2O)/Q_{\mathrm{rot}}(0\rightarrow1,H_2O)$ is 1.11 at 1 eV and 1.17 at 0.1 eV. It should be noted here that, as for the isotope effect, they took into account only the difference in the rotational constant. They assumed the same interaction potential for the two isotopes. Actually, D_2O has almost the same value of dipole moment as H_2O.[14] The remaining difference in the interaction may not much affect the dipole allowed transition (say, $J=0\rightarrow1$), but change the result for other transitions (i.e., $J=0\rightarrow0,2,3,\ldots$).

6. Vibrational Excitation

To date three electron beam/gas beam measurements[45–47] of vibrational excitation cross section, Q_{vib}, have been reported. None was capable of resolving the two stretching modes, (100) and (001). Hence everyone gave the cross section for the composite of the two modes. (Recently, however, a new experiment has reported separate excitation cross sections for the two stretching modes albeit at one angle and three energies. See below.) The results of these three measurements are almost in agreement with one another for the stretching modes. Taking a weighted average of those data, Brunger *et al.*[49] have determined the recommended values of Q_{vib} in the energy range 1–20 eV (Fig. 9). For the bending mode, there are some discrepancies between the results of the three measurements. In particular, El-Zein *et al.*[48] found a resonance-like sharp peak at 7.5 eV for the (010) excitation. Placing a more weight on the most recent result by

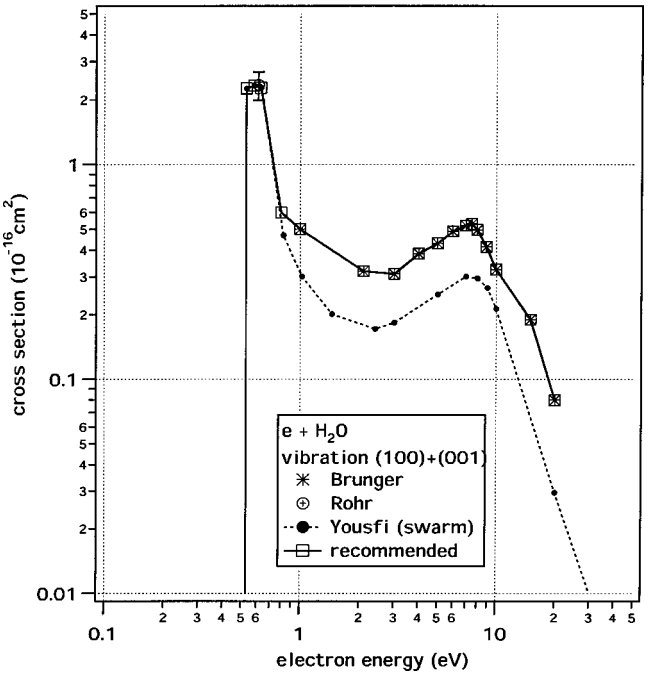

FIG. 9. Cross sections for the vibrational excitation of stretching modes of H_2O. The present recommended values are compared with those recommended by Brunger *et al.* (Ref. 49), experimental data obtained by Yousfi and Benabdessadok (Ref. 40), and Rohr (Ref. 53).

El-Zein *et al.*,[48] Brunger *et al.*[49] have determined the recommended values of Q_{vib} for the (010) mode as shown in Fig. 10.

Three different groups[50–52] have published theoretical calculations of Q_{vib} for H_2O. None of the theoretical calcula-

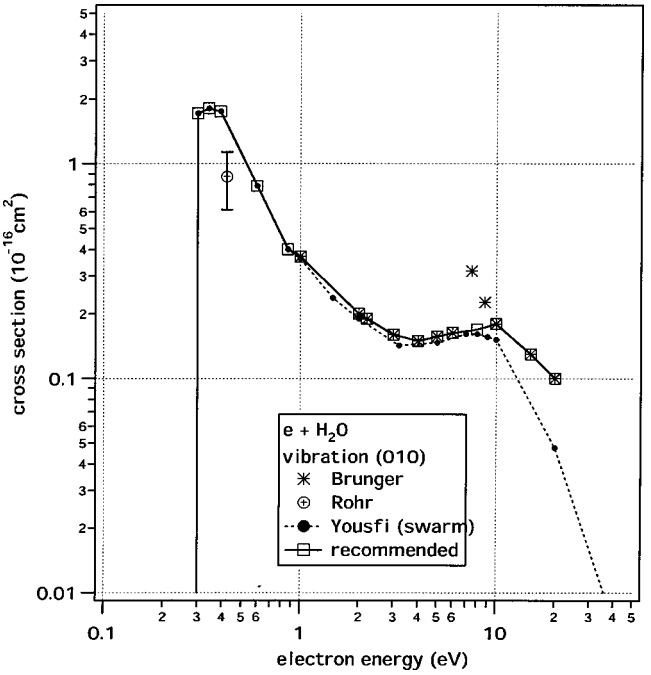

FIG. 10. Cross sections for the vibrational excitation of bending mode of H_2O. (See Fig. 9 for the references.)

tions show any evidence for the resonance-like structure at 7.5 eV. The DCS for the (010) excitation calculated at 7.8 eV by Moreira *et al.*,[52] for example, shows a significant difference from the corresponding values of El-Zein *et al.*, but agrees with the other two experiments. Further, preliminary results of recent measurements by Danjo *et al.* (private communication) and Tanaka *et al.* (private communication) show no evidence of the resonance. Considering these facts, we cannot discard the possibility that the sharp peak of El-Zein *et al.* at 7.5 eV is an artifact. Thus, we have constructed our recommended cross section without including the peak of (010) cross section of El-Zein *et al.* We have modified the recommended cross sections of Brunger *et al.*[49] in such a way as shown in Figs. 9 and 10.

Seng and Linder[45] obtained a sharp peak in their cross sections near the respective threshold. Rohr[53] repeated the measurement in the threshold region and found somewhat different results from Seng and Linder. Rohr does not report the energy dependence of ICS, but only the peak values [23.4×10^{-17} cm^2 at 0.61 eV for (100)+(001) transition and 8.7×10^{-17} cm^2 at 0.42 eV for (010) mode].

From a swarm analysis, Yousfi and Benabdessadok[40] derived Q_{vib} over a wide range of electron energies. Their result is plotted in Figs. 9 and 10. In the energy region above 1 eV, the swarm data agree with the present recommended values for (010) transition, but not for (100)+(001). In principle, the swarm data are more reliable in the lower energy region. Here we adopt the swarm data to extend the recommended values to the energies below 1 eV. The resulting Q_{vib} for the stretching modes is consistent with the peak found by Rohr, but it does not hold for the bending mode. Recently Nishimura and Gianturco[54] repeated the calculation of Nishimura and Itikawa[51] with an improved potential for electron-exchange and polarization interactions. Particularly they obtained theoretical cross sections at the energies below 1 eV. Their result for the bending mode is in good agreement with the present recommended values. Their cross sections for the stretching modes, however, do not reproduce the experimental peak observed by Rohr and disagree with the present recommended values over the whole energy range up to 10 eV.

Allan and Moreira[55] recently succeeded to separately measure the cross sections for the two stretching modes, (100) and (001). They reported only the DCS at 135° measured at the energies of 0.05, 0.6, and 3.0 eV above the respective thresholds. They found that, at all the energies of their experiment, the symmetric stretching mode, (100), has much larger cross sections than the antisymmetric one, (001). Nishimura and Gianturco[54] found a similar trend in their calculation. For example, the excitation cross section for (100) calculated by Nishimura and Gianturco at 1 eV is about four times larger than the corresponding value for (001). It should be noted that Nishimura and Gianturco report only ICS and, hence, no direct comparison with the experimental DCS can be made.

Allan and Moreira[55] also reported the cross section for the vibrational excitation of D_2O. Their measured cross sections (i.e., DCS at 135° and at 0.6 eV above the threshold) show a small isotope effect. The cross section for H_2O is larger than that for D_2O for all the three normal modes. For the stretching modes, this is almost consistent with a previous measurement of isotope effect by Ben Arfa *et al.*[56] The latter authors measured the DCS at 40° and 8 eV. They observed no isotopic difference for the bending mode. Since the nuclear motion is directly involved, the study of isotope effect must be valuable in the understanding of the vibrational excitation of molecules.

Having reviewed all the data, our recommended values of Q_{vib} are given in Table 9, nevertheless we recommend that new experimental data be collected, both DCS and ICS for vibrational excitation of H_2O.

TABLE 9. Recommended vibrational excitation cross sections for $e+H_2O$

(100)+(001)		(010)	
Energy (eV)	Cross section (10^{-16} cm^2)	Energy (eV)	Cross section (10^{-16} cm^2)
0.453	0	0.198	0
0.53	2.25	0.3	1.71
0.58	2.32	0.34	1.805
0.63	2.27	0.39	1.748
0.8	0.6	0.6	0.7885
1	0.500	0.862	0.399
2.1	0.320	1	0.370
3	0.310	2	0.200
4	0.385	2.2	0.190
5	0.430	3	0.160
6	0.489	4	0.150
7	0.520	5	0.157
7.5	0.529	6	0.163
8	0.495	8	0.17
8.875	0.413	10	0.180
10	0.325	15	0.130
15	0.190	20	0.100
20	0.080		

7. Excitation of Electronic States

7.1. Excited States

Table 10 lists the electronically excited states of H_2O below about 11 eV. The electronically ground state of H_2O belongs to the C_{2v} symmetry and has the electron configuration

$$(1a_1)^2(2a_1)^2(1b_2)^2(3a_1)^2(1b_1)^2.$$

Table 10 shows the vertical excitation energies for each excited state. Each excited state is labeled by the irreducible representation of the C_{2v} group (the first column of the table) and the dominant excitation from the ground state (the second column). The standard way to study excited states is through photoabsorption spectroscopy. However, the most recent spectroscopic study of H_2O is that of Chan *et al.*,[57] who employed the dipole (e,e) method (see below) to mimic a photoabsorption spectra. Excitation energies derived from their spectra are listed in the seventh column of Table 10. The spectrum of water in the energy region 10–20 eV con-

TABLE 10. Electronically excited states of H_2O. Vertical excitation energies are shown in eV

State	Excitation	Chujian[a]	Winter[b]	van Harrevelt[c]	Gorfinkiel[d]	Chan[e]
$4\,^1A_1$ ($\tilde{F}$)	b_1-3db$_1$	11.13		11.16 ($5A'$)[f]		11.057
$1\,^1B_2$	b_1-3da$_2$	11.1		11.11 ($4A'$)		
$4\,^1B_1$ ($\tilde{E}$)	b_1-3da$_1$	11.01				10.990
$2\,^1A_2$	b_1-3db$_2$	10.84		11.02 ($4A''$)		
$2\,^3A_2$	b_1-3db$_2$	10.68				
$3\,^1B_1$	b_1-4sa$_1$	10.52				
$3\,^3B_1$	b_1-4sa$_1$	10.39				
$3\,^1A_1$ ($\tilde{D}$)	b_1-3pb$_1$	10.16	10.16	10.11 ($3A'$)		10.171
$2\,^1B_1$ ($\tilde{C}$)	b_1-3pa$_1$	10.01	10.06	10.11 ($3A''$)		9.994
$2\,^3B_1$ ($\tilde{c}$)	b_1-3pa$_1$	9.98	9.99			
$2\,^3A_1$ ($\tilde{d}$)	b_1-3pb$_1$	9.81	9.74			
$2\,^1A_1$ ($\tilde{B}$)	$3a_1$-3sa$_1$	9.7	9.82	9.95 ($2A'$)	9.86	9.7
$1\,^3A_1$ ($\tilde{b}$)	$3a_1$-3sa$_1$	9.3	9.44		9.20	
$1\,^1A_2$	b_1-3pb$_2$	9.1	9.46	9.60 ($2A''$)		
$1\,^3A_2$	b_1-3pb$_2$	8.9	9.34			
$1\,^1B_1$ ($\tilde{A}$)	b_1-3sa$_1$	7.4	7.61	7.63 ($1A''$)	7.51	7.4
$1\,^3B_1$ ($\tilde{a}$)	b_1-3sa$_1$	7.0	7.26		7.03	
$1\,^1A_1$ ($\tilde{X}$)		0.0	0.0	0.0 ($1A'$)	0.0	0.0

[a]Electron energy loss spectra.[59]
[b]*ab initio* calculation.[61]
[c]Theoretical potential energy surface.[62]
[d]Theoretical potential energy surface.[28]
[e]"Equivalent" photoabsorption spectroscopy with the dipole (e,e) method.[57]
[f]Notation of C_s symmetry.

sists of many discrete peaks, which may be assigned to the transitions from the outer valence to the Rydberg orbitals. The Rydberg series of the spectra has been analyzed in detail by Gürtler *et al.*[58]

The photoabsorption spectroscopy only gives information on the optically allowed excited states. Electron-impact spectroscopy is useful for the study of optically forbidden states. The most extensive work of electron spectroscopy of H_2O was made by Chutjian *et al.*[59] They covered the energy loss range of 4.2–12 eV. With the help of *ab initio* calculations,[60,61] Chutjian *et al.* assigned their energy loss peaks as shown in Table 10. The third column of the table lists the transition energies measured by Chutjian *et al.*

To study the detailed structure of the excited states, we have to know the nuclear configuration dependence of the excitation energy, i.e., the potential surfaces. Recently van Harrevelt and van Hemert[62] have made an elaborate *ab initio* calculation of the potential surfaces of H_2O. States of H_2O with its arbitrary nuclear configuration are denoted by the irreducible representation (A' and A'') of the C_s group. Using the multireference configuration interaction method, van Harrevelt and van Hemert calculated the potential surfaces for the four lowest states of both A' and A'' symmteries. Their result of the vertical excitation energies are shown in the fifth column of Table 10. They considered only the spin-singlet states. In order to calculate excitation cross section, Gorfinkiel *et al.*[28] theoretically constructed the potential surfaces of H_2O. They changed the length of one OH bond, but fixed the other OH bond and the H–O–H angle at their equilibrium values. They considered the lowest two excited states of both A' and A'', and both singlet and triplet states. The transition energies of their lowest four states are given in the sixth column of Table 10 and they are in good agreement with experimental values. The four higher energy states are located too high compared with the experimental result. This may be due to the fact that diffuse states cannot be accurately represented in their calculation.

7.2. Excitation Cross Sections

To date no electron beam measurements have reported absolute values of the excitation cross section of H_2O. Therefore to provide information on the excitation cross sections of water, data have, at present, to be based upon: a semiempirical model, a swarm experiment and theory. Taking into consideration the results of photoabsorption and electron-impact spectroscopies, Olivero *et al.*[63] introduced a semiempirical model to produce a set of excitation cross sections of H_2O. Zaider *et al.*[64] modified those cross sections to apply them to the track structure calculation in radiobiology. Yousfi and Benabdessadok[40] made a swarm experiment and derived a cross section set for H_2O. For the excitation of electronic states, they used the work of Olivero *et al.* to determine excitation processes and their threshold energies. Those excitation processes, however, do not necessarily correspond to those listed in Table 10. For example, they assumed a triplet state excitation with the threshold of 4.5 eV. A detailed measurement of the energy loss spectra in the 4–6 eV region by Edmonson *et al.*[65] and later by Cvejanovic *et al.*[66] confirmed no state at around 4.5 eV. Instead, as is shown in Table 10, we have the $^3B_1$ state at 7.0 eV, which was not taken into account in the swarm analysis.

There are five theoretical papers reporting excitation cross sections of H_2O.[28,67–70] All of them, except that of Gorfinkiel *et al.*, based their calculation on the fixed-nuclei approximation. Gorfinkiel *et al.*[28] sought to take into account the nuclear motion. All of the five papers report the cross section for the excitation of $\tilde{b}\ ^3A_1(3a_1-3sa_1)$ state. Three of them[28,66,68] also present the cross section for the excitation of $\tilde{a}\ ^3B_1(b_1-3sa_1)$, $\tilde{A}\ \ 1\,^1B_1(b_1-3sa_1)$, and $\tilde{B}\ 2\,^1A_1(3a_1-3sa_1)$ states. As shown by Gorfinkiel *et al.*, the resulting theoretical cross sections show significant differences. Furthermore, there is a significant difference between the cross sections calculated with and without nuclear motion considered. In principle the calculation including nuclear motion should be more accurate than the others. Since the method of Gorfinkiel *et al.* was, however, very approximate, no definite conclusions can be drawn as to the behavior of the excitation cross section. Theoretical cross sections show the Feshbach resonance (for details, see Gorfinkiel *et al.*[28]). They are closely related with the onset of dissociative attachment observed (see Sec. 9). Gorfinkiel *et al.* showed, however, that the theoretical behavior of the resonance depends on how to treat the nuclear motion in the calculation.

A measurement of electron energy-loss spectra has a possibility of providing DCS for the excitation process. Trajmar *et al.*[71] measured the energy loss spectra at the electron energies of 15, 20, and 53 eV. They derived DCS for a number of excited states but only in relative scale. From a beam experiment at 500 eV, Lassettre *et al.*[72] obtained the generalized oscillator strength (GOS) for the energy loss peak at 7.4, 10.1, 11.0, and 13.3 eV over the squared momentum transfer $K^2=0.1-2.0$ a.u. Klump and Lassettre[73] extended the measurement and determined the GOS for the 7.4 eV peak up to $K^2=4.5$ a.u. According to the Born–Bethe theory, an intensity at the forward scattering for incident energy much higher than 100 eV gives the optical oscillator strength. This is called the dipole (e,e) method. To obtain the ''equivalent'' photoabsorption spectrum of H_2O with this method, Chan *et al.*[57] measured the forward angle electron scattering with 8 keV electrons. Such information, though fragmentary, may be useful in the testing of theoretical calculations.

Due to the lack of data, we therefore cannot provide a recommended set of values for electron impact excitation of water. This is a serious problem since electronic excitation is important in planetary atmospheres, plasmas, and radiation chemistry. Experiments and refined theory are urgently needed.

8. Ionization

Recently Lindsay and Mangan[74] reviewed available experimental data on the electron impact ionization cross section of molecules. In so doing, they put much stress on the reliability of the experimental techniques employed. In particular, methods capable of collecting all the product ions are preferred. A special care should be taken to avoid discrimination against energetic fragment ions. Furthermore, a greater weight is placed on the experiment not relying on normalization to other works. As a result, Lindsay and Mangan[74] have

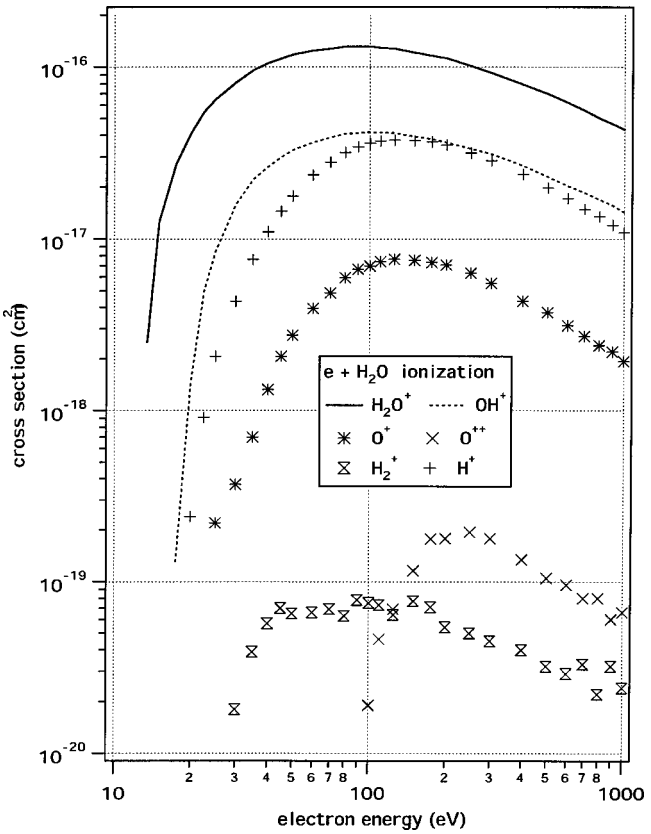

FIG. 11. Recommended values of the partial ionization cross sections of H_2O for the production of H_2O^+, OH^+, O^+, O^{++}, H_2^+, and H^+.

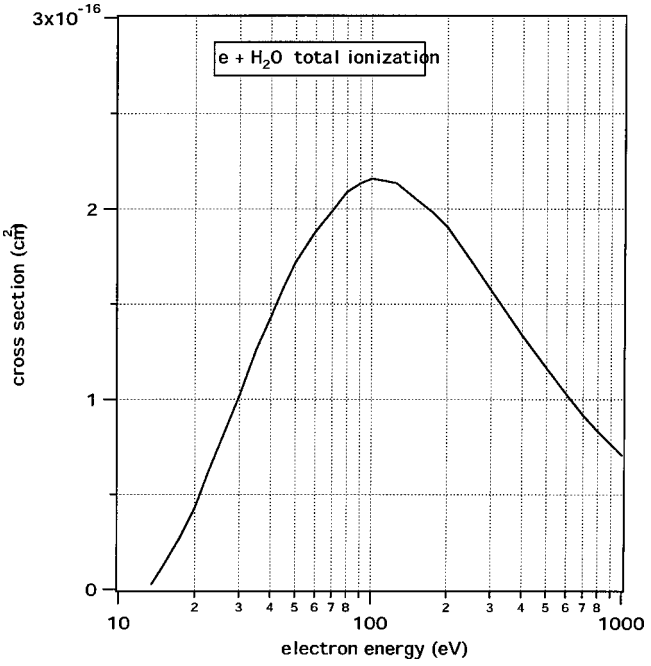

FIG. 12. Recommended values of total ionization cross section of H_2O.

TABLE 11. Recommended ionization cross sections for $e + H_2O$

Energy (eV)	H_2O^+ (10^{-16} cm^2)	OH^+ (10^{-16} cm^2)	O^+ (10^{-18} cm^2)	O^{++} (10^{-18} cm^2)	H_2^+ (10^{-18} cm^2)	H^+ (10^{-16} cm^2)	Total (10^{-16} cm^2)
13.5	0.025						0.025
15	0.126						0.126
17.5	0.272	0.0013					0.274
20	0.411	0.0145				0.0024	0.428
22.5	0.549	0.0500				0.0091	0.609
25	0.652	0.0855	0.22			0.0207	0.761
30	0.815	0.160	0.37		0.018	0.0433	1.02
35	0.958	0.222	0.70		0.039	0.0759	1.26
40	1.05	0.264	1.32		0.057	0.110	1.43
45	1.12	0.300	2.07		0.070	0.145	1.59
50	1.18	0.329	2.75		0.065	0.178	1.72
60	1.24	0.364	3.94		0.066	0.235	1.88
70	1.27	0.389	4.84		0.069	0.279	1.99
80	1.31	0.409	5.94		0.063	0.317	2.09
90	1.31	0.412	6.66	0.008	0.078	0.343	2.13
100	1.31	0.418	6.95	0.019	0.075	0.360	2.16
110	1.29	0.415	7.38	0.046	0.073	0.370	2.15
125	1.27	0.412	7.63	0.069	0.064	0.375	2.13
150	1.21	0.393	7.52	0.116	0.077	0.371	2.05
175	1.16	0.381	7.31	0.178	0.071	0.366	1.99
200	1.12	0.363	7.07	0.179	0.054	0.351	1.90
250	1.01	0.334	6.34	0.195	0.050	0.316	1.73
300	0.921	0.311	5.51	0.179	0.045	0.284	1.57
400	0.789	0.266	4.34	0.134	0.040	0.237	1.34
500	0.696	0.230	3.73	0.105	0.032	0.198	1.16
600	0.618	0.203	3.13	0.096	0.029	0.172	1.02
700	0.555	0.185	2.71	0.080	0.033	0.149	0.917
800	0.502	0.169	2.40	0.080	0.022	0.135	0.830
900	0.465	0.156	2.20	0.060	0.032	0.120	0.763
1000	0.432	0.143	1.94	0.066	0.024	0.109	0.705

determined the recommended values of ionization cross section for H_2O on the basis of the measurement by Straub *et al.*[75]

Straub *et al.* used a parallel plate apparatus with a time-of-flight mass spectrometer and position sensitive detector of product ions. The partial ionization cross sections were made absolute independently, i.e., without resorting to any normalization procedure. Lindsay and Mangan slightly corrected the original values of Straub *et al.* considering a recent recalibration of their apparatus. The recommended cross section was reported each for the product ions, H_2O^+, OH^+, O^+, O^{++}, H_2^+, H^+. Those are shown in Fig. 11. We therefore recommend these values noting that, according to Lindsay and Mangan, the uncertainties of the partial cross sections are 6%, 7%, 9%, 13%, 16%, and 6.5% for the H_2O^+, OH^+, O^+, O^{++}, H_2^+, and H^+ ions, respectively. The uncertainty in the electron energy is ± 1 eV. Though the production of H_2O^{++} has been reported by Rao *et al.*,[76] Straub *et al.* had no evidence of that. They estimated the cross section for H_2O^{++} to be less than 10^{-20} cm^2 at 200 eV. The total ionization cross section was obtained as a sum of those partial ones. The uncertainty of that is 6%. The resulting values (shown in Fig. 12) are in good agreement with those obtained by a total-ion-current measurement (e.g., Schutten *et al.*[77]) within the combined error limit and theoretical cross sections obtained with the BEB method by Hwang *et al.*[78] The total and partial

TABLE 12. Single differential cross section for ionization of H_2O (in 10^{-19} cm^2/eV)

	Incident electron energy (eV)					
E_s (eV)[a]	50	100	200	300	500	1000
2	240	250	210	160	110	65
4	170	160	130	110	70	41
6	130	120	100	85	57	30
8	110	93	80	66	44	24
10	92	74	69	53	36	20
14	71	50	47	38	26	14
20	66	32	28	22	16	9.0
25	81	24	20	16	12	6.5
34	140	18	12	9.6	6.9	4.1
40		17	9.7	7.0	5.1	3.3
48		18	6.9	5.2	3.8	2.3
56		22	5.4	3.9	2.7	1.7
70		36	4.3	2.5	1.8	1.1
100			4.0	1.4	0.87	0.55
150			11	1.2	0.40	0.25
200				2.5	0.28	0.16
240				5.6	0.26	0.11
300					0.38	0.074
400					0.14	0.056
500						0.050
700						0.095

[a]Energy of secondary electron.

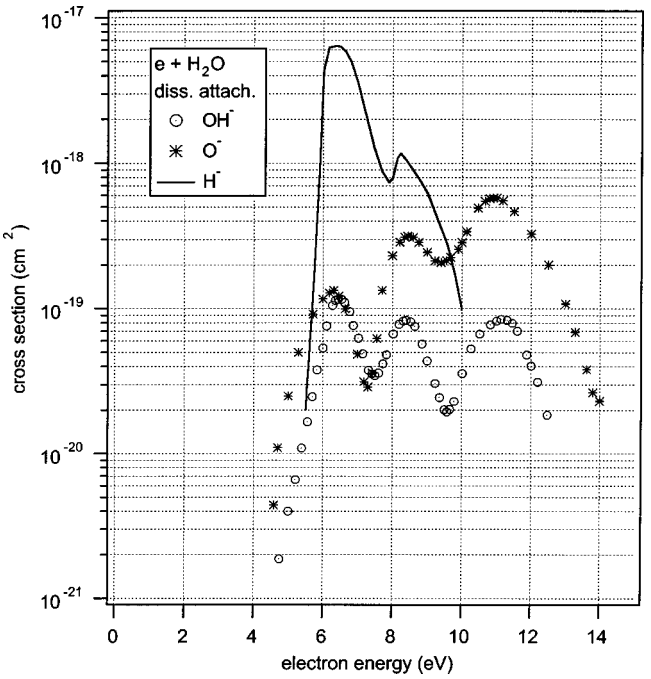

FIG. 13. Recommended values of the electron attachment cross sections of H_2O for the production of OH^-, O^-, and H^-.

TABLE 13. Recommended cross sections for production of H^- from H_2O

Energy (eV)	Cross section (10^{-18} cm^2)
5.5	0.02
5.74	0.16
5.9	0.985
6.01	4.3
6.165	6.22
6.286	6.317
6.4	6.37
6.52	6.25
6.65	5.79
6.81	4.89
7.0	3.56
7.465	1.29
7.69	0.877
7.89	0.74
8.0	0.79
8.09	0.995
8.14	1.09
8.235	1.166
8.395	1.04
8.79	0.76
9.01	0.62
9.57	0.28
9.8	0.17
10.0	0.098

ionization cross sections shown here are presented in Table 11.

The appearance potential of each fragment ion was measured independently as

$e + H_2O \rightarrow H^+$	16.95 ± 0.05 eV,[79]
OH^+	18.116 ± 0.003 eV,[14]
O^+	19.0 ± 0.2 eV,[80]
H_2^+	20.7 ± 0.4 eV.[80]

In Table 11, the cross section for OH^+ has a nonzero value at 17.5 eV. This seems contradictory to the appearance potential shown here (i.e., 18.116 eV). This discrepancy is probably due to the uncertainty in the energy of the electron beam mentioned above.

The energy distribution of the ejected (secondary) electrons is of practical importance. It is needed when the energy deposition of the incident electron is required, e.g., in models of radiation damage where the secondary electrons lead to strand breaks in cellular DNA. The energy distribution, called the single differential cross section (SDCS) of ionization, was obtained experimentally by Bolorizadeh and Rudd.[81] They measured angular distribution of the ejected electrons, from which the SDCS was derived. Their values of SDCS are shown in Table 12. More detailed information of angular and energy distributions of the ejected electrons can be found in a recent theoretical paper by Champion *et al.*[82]

On the basis of the measurements of several groups, Lindsay and Mangan concluded that the H_2O and D_2O total and partial ionization cross sections are essentially identical. Recently Tarnovsky *et al.*[83] measured the partial cross sections for the production of D_2O^+, OD^+, and D^+ from D_2O. Their result is consistent with those of Lindsay and Mangan, at least within the somewhat large error bars.

9. Dissociative Attachment

Electron attachment to many molecules has been reviewed by Itikawa.[84] For H_2O, he selected the cross section mea-

TABLE 14. Recommended cross sections for production of O^- from H_2O

Energy (eV)	Cross section (10^{-18} cm^2)	Energy (eV)	Cross section (10^{-18} cm^2)
4.43	0	9	0.244
4.59	0.0044	9.22	0.213
4.71	0.011	9.4	0.208
5	0.025	9.56	0.214
5.29	0.05	9.67	0.226
5.72	0.0913	9.89	0.256
6	0.116	10	0.285
6.19	0.128	10.138	0.337
6.32	0.133	10.46	0.493
6.45	0.122	10.66	0.55
6.64	0.1	10.8	0.57
7	0.0485	10.9	0.576
7.186	0.0313	11	0.576
7.3	0.0287	11.18	0.553
7.43	0.036	11.5	0.466
7.56	0.062	12	0.327
7.7	0.133	12.5	0.2
8	0.23	13	0.108
8.21	0.286	13.28	0.0688
8.35	0.31	13.625	0.038
8.44	0.316	13.8	0.0264
8.6	0.31	14	0.023
8.76	0.285		

TABLE 15. Recommended cross sections for production of OH^- from H_2O

Energy (eV)	Cross section (10^{-18} cm^2)	Energy (eV)	Cross section (10^{-18} cm^2)
4.3	0	8.19	0.078
4.51	9*e*-04	8.31	0.082
4.75	1.87*e*-03	8.385	0.083
5.0	4*e*-03	8.53	0.081
5.21	6.6*e*-03	8.64	0.0756
5.39	0.0109	8.85	0.057
5.56	0.0165	9.0	0.0436
5.69	0.0246	9.23	0.0304
5.836	0.0379	9.36	0.0244
6.0	0.0537	9.49	0.0201
6.1	0.0757	9.57	0.0194
6.27	0.1048	9.654	0.0202
6.36	0.114	9.78	0.0229
6.437	0.116	10.01	0.0358
6.536	0.1154	10.26	0.053
6.626	0.1105	10.52	0.066 86
6.77	0.095	10.825	0.0775
6.874	0.0763	11.0	0.082 35
7.02	0.062 35	11.13	0.0847
7.15	0.0489	11.3	0.083
7.32	0.0376	11.45	0.0795
7.413	0.0356	11.6	0.0699
7.49	0.0345	11.87	0.048 18
7.6	0.036	12.0	0.0402
7.73	0.0417	12.19	0.0311
7.83	0.048	12.47	0.0184
8.02	0.067		

sured by Melton[85] as a recommended value, since Melton's cross section shows a good agreement with the result of a previous independent measurement by Compton and Christophorou[86] and no recent measurement of the absolute values of the cross section has been reported. We confirm this recommendation.

Electron attachment to water results in three kinds of negative ion fragments, H^-, O^-, and OH^-. Cross sections for each anion are shown in Fig 13. Their numerical values are given in Tables 13, 14, and 15. Belic *et al.*[87] made a detailed study of the attachment process (e.g., measurements of energy and angular distributions of H^-). They interpreted the three peaks in the cross sections (at 6.5, 8.6, and 11.8 eV) as being due to the Feshbach resonances. (Melton showed no third peak in the H^- curve. Belic *et al.*, however, observed H^- at around 11.8 eV and concluded its intensity to be approximately 600 times weaker than the value at 6.5 eV.) The three peaks correspond to the resonance with $^3B_1$ (at 7.0 eV), $^3A_1$ (9.3 eV), and $^3B_2$ ($\sim$12.3 eV) as a parent, respectively. Their electronic configurations would be $(1b_1)^{-1}(3sa_1)^2\ ^2B_1$, $(3a_1)^{-1}(3sa_1)^2\ ^2A_1$, and $(1b_2)^{-1}(3sa_1)^2\ ^2B_2$. Jungen *et al.*[88] calculated the resonance energies of the states and obtained reasonable agreement with the experimental results. These Feshbach resonances might affect other collision processes (i.e., elastic scattering and excitations of rotational, vibrational, and electronic states). There is however no report of experimental observation of these resonances in elastic and vibrational cross sections, but theoretical calculations of electron-impact excitation of electronic states suggest that these Feshbach resonances may be observed in excitation cross section (see, for example, Gorfinkiel *et al.*[28]).

TABLE 16. Dissociation channels of H_2O produced by electron impact

Dissociation products	Minimum energy (eV)	Observed threshold (eV)
$O(^3P)+H_2(X)$	5.03	
$OH(X)+H(n=1)$	5.10	7.0[a]
$O^*(^1D)+H_2(X)$	7.00	
$OH^*(A)+H(n=1)$	9.15	9.0 ± 0.3[b]
$O^*(^1S)+H_2(X)$	9.22	15.5 ± 1.0[c]
$O(^3P)+2\,H$	9.51	
$O^*(3s\ ^3S^o)+H_2(X)$	14.56	23.5[d]
$OH(X)+H^*(n=2)$	15.30	15.4[d]
$OH(X)+H^*(n=3)$	17.19	18.5 ± 0.5[b]

[a]Observed by Harb *et al.*[101]
[b]Observed by Beenakker *et al.*[92]
[c]Observed by Kedzierski *et al.*[100]
[d]Observed by Morgan and Mentall.[96]

In recommending the values of Melton, we remark that these are over 30 years old and it is now known that many early measurements of anions produced by electron impact suffered from kinetic energy discrimination of the anions. We therefore strongly recommend a new measurement of dissociative electron attachment to water.

Dissociative attachment is expected to have a large isotope effect. Compton and Christophorou[86] have measured dissociative attachment cross section both for the D^- formation from D_2O and for the H^- formation from H_2O. They found that the ratio of the D^- cross section to the H^- one was 0.75 at the maximum (at 6.5 eV). The corresponding ratio for the energy-integrated cross section was 0.60. This is easily understood by the large mass of D^- compared with H^-. (A more detailed discussion of this isotope effect is given by Belic *et al.*[87]) Compton and Christophorou showed no absolute values of cross section for the O^- production. They only indicated that the relative magnitudes of the three peaks in the O^- cross section were different depending on the targets, H_2O or D_2O.

10. Emission Cross Sections

When an electron collides with a water molecule, radiation is emitted over a wide range of wavelengths. Most of the radiation arises from dissociation fragments in their excited states (i.e., H*, O*, OH*). The corresponding emission cross sections, Q_{emis}, are discussed here in two spectral regions: (1) visible and near ultraviolet (UV) regions and (2) vacuum ultraviolet (VUV) region. Table 16 summarizes the possible dissociation channels in electron impact with water. It shows the minimum energy for the formation of the respective fragments (according to the thermodynamics given in Sec. 2) with the corresponding thresholds observed in experiments.

One of the important aspects of the emission measurement is the degree of polarization of the radiation. To accurately determine the emission cross section, one has to take into

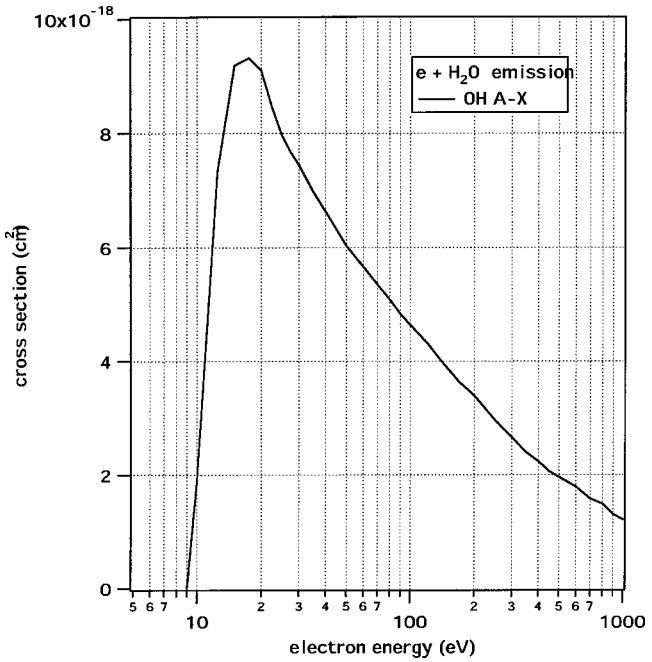

FIG. 14. Cross sections for the emission of OH $A-X$ bands upon electron collisions with H_2O, measured by Beenakker *et al.* (Ref. 92).

account the polarization of the emission. All of the experiments cited below, however, assume the polarization to be weak or simply ignore the effect. There is a measurement of polarization for the emission of OH A-X transition. Becker *et al.*[89] found the polarization of its (0,0) band is -5.2 $(\pm 1.1)\%$ at 11.9 eV, but becomes less than a few % at the energies above 20 eV. For the Balmer radiation, Vroom and de Heer[90] could not detect any polarization at least above 50 eV. Furthermore, the VUV emission following dissociative excitation of polyatomic molecules can be assumed unpolarized, because a large number of repulsive channels are involved in the process.[91] In any case, considering the uncertainty of the measured values of Q_{emis}, the polarization of the emission, if any, does not affect the conclusion presented below about the emission cross section.

TABLE 17. Cross section for the $A-X$ emission from OH in dissociation of H_2O by electron impact, measured by Beenaker *et al.*[92]

Energy (eV)	Cross section (10^{-18} cm^2)	Energy (eV)	Cross section (10^{-18} cm^2)
9	0	100	4.64
10	1.87	120	4.32
12.5	7.33	140	4.00
15	9.19	170	3.64
17.5	9.32	200	3.39
20	9.11	250	2.97
22.5	8.45	300	2.66
25	7.97	350	2.40
27.5	7.67	400	2.24
30	7.45	450	2.06
35	6.98	500	1.96
40	6.63	600	1.79
50	6.03	700	1.58
60	5.66	800	1.49
70	5.35	900	1.31
80	5.08	1000	1.21
90	4.83		

TABLE 18. Emission cross sections produced by electron impact in H_2O at 100 eV (in 10^{-18} cm^2)

Transition	Beenakker[92]	Möhlmann[94]	Müller[93]
OH $A-X$	4.64 (0.87)[a]		2.7 (0.4)
H 3–2		3.55 (0.43)	2.7 (0.4)
H 4–2	0.641 (0.064)	0.683 (0.082)	0.49 (0.07)
H 5–2		0.273 (0.055)	0.19 (0.03)
H 6–2		0.102 (0.020)	0.089 (0.013)
O 777.4	0.126 (0.025)		
O 844.7	0.286 (0.057)		

[a]The numbers in the parentheses are the possible errors estimated.

10.1. Visible and Near-UV Regions

There are two comprehensive studies of the spectra in this region,[92,93] and earlier measurements are reviewed in these two papers. Beenakker *et al.*[92] measured the emission in the 185–900 nm region. They obtained the Q_{emis} at the collision energies from threshold to 1000 eV. Müller *et al.*[93] surveyed the emission in the 280–500 nm region, but reported an absolute cross section only at 100 eV.

OH* $A-X$ Transition

Beenakker *et al.*[92] assigned the emission in the 306–350 nm region as the transition

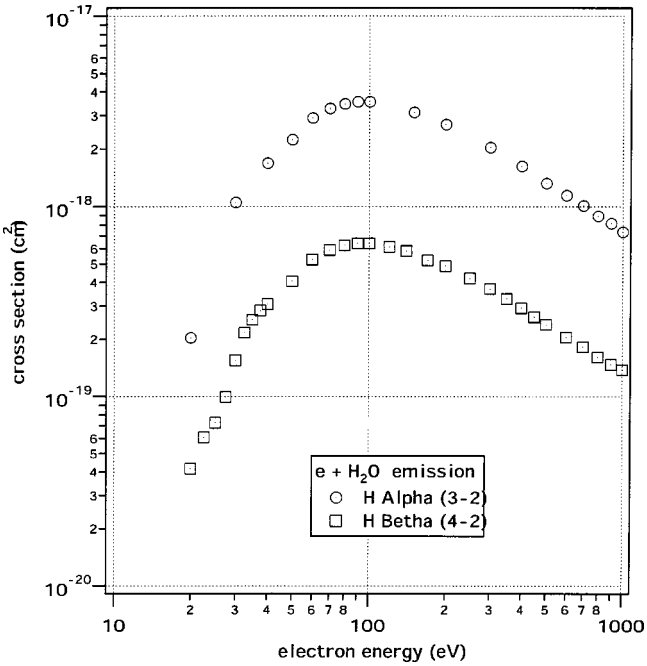

FIG. 15. Cross sections for the emission of H Balmer α radiation (measured by Möhlmann and de Heer, Ref. 94) and H Balmer β radiation (measured by Beenakker *et al.*, Ref. 92).

TABLE 19. Cross section for the emission of H Balmer α (3–2) line produced by electron impact dissociation of H_2O, measured by Möhlmann and de Heer[94]

Energy (eV)	Cross section (10^{-18} cm^2)
20	0.204
30	1.05
40	1.69
50	2.24
60	2.91
70	3.26
80	3.46
90	3.54
100	3.55
150	3.11
200	2.69
300	2.04
400	1.62
500	1.32
600	1.14
700	1.01
800	0.892
900	0.814
1000	0.734

OH (0–0, 1–1, 2–2) bands of $A\,^2\Sigma^+ - X\,^2\Pi$.

The cross section for the emission they measured is shown in Fig. 14 and listed in Table 17. Beenakker *et al.* estimated an uncertainty of 19% at 300 eV. A similar measurement was performed later by Müller *et al.*[93] They resolved each of 0–0, 1–1, and 2–2 bands. The cross section summed over the three bands at the collision energy of 100 eV is compared in Table 18 with the corresponding value obtained by Beenakker *et al.* Despite the uncertainty claimed in both the experiments, the two experimental cross sections differ markedly from one another.

H* Balmer Emissions

Beenakker *et al.*[92] measured the cross sections for the Balmer emissions

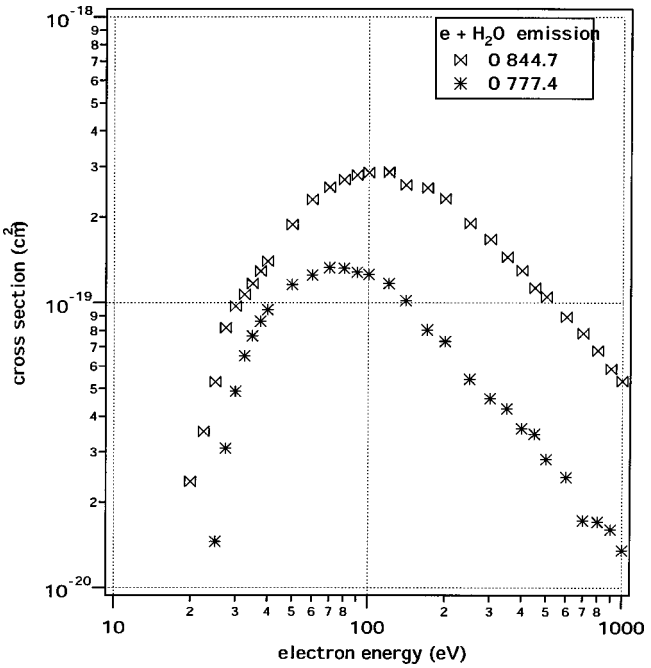

FIG. 16. Cross sections for the emissions of the O 3p ^{3}P–3s ^{5}S^o transition at 777.4 nm and O 3p ^{5}P–3s ^{3}S^o transition at 844.7 nm, measured by Beenakker *et al.* (Ref. 92).

H $n=3-2$ at 656.3 nm,
$n=4-2$ at 486.1 nm,
$n=5-2$ at 434.0 nm,
$n=6-2$ at 410.2 nm.

They reported the energy dependence of the Q_{emis} only for the Balmer β $(n=4-2)$ emission and this is shown in Fig. 15. From the measurement at 100, 200, 500, and 800 eV, they concluded that the energy dependence of all the Balmer lines is the same within 4%. They reported the Q_{emis} at 300 eV for all the Balmer lines relative to the Balmer β one. The Q_{emis} for the Balmer radiation has also been measured by Möhlman and de Heer.[94] They showed the energy depen-

TABLE 20. Cross section for the emissions of H Balmer β, O 844.7, and O 777.4 lines upon $e+$ H_2O collisions, measured by Beenakker *et al.*[92]

Energy (eV)	H β (4–2) (10^{-19} cm^2)	O 844.7 (10^{-19} cm^2)	O 777.4 (10^{-19} cm^2)	Energy (eV)	H β (4–2) (10^{-19} cm^2)	O 844.7 (10^{-19} cm^2)	O 777.4 (10^{-19} cm^2)
20	0.415	0.236	0.035	120	6.13	2.87	1.17
22.5	0.607	0.354	0.078	140	5.83	2.59	1.02
25	0.726	0.528	0.145	170	5.22	2.53	0.804
27.5	0.991	0.818	0.308	200	4.86	2.32	0.734
30	1.55	0.972	0.489	250	4.18	1.90	0.540
32.5	2.17	1.07	0.653	300	3.68	1.67	0.461
35	2.54	1.17	0.765	350	3.27	1.45	0.425
37.5	2.84	1.29	0.861	400	2.92	1.30	0.362
40	3.06	1.40	0.945	450	2.62	1.13	0.347
50	4.04	1.88	1.16	500	2.39	1.05	0.282
60	5.25	2.30	1.29	600	2.05	0.892	0.244
70	5.89	2.54	1.33	700	1.82	0.784	0.172
80	6.25	2.70	1.32	800	1.61	0.680	0.170
90	6.40	2.80	1.28	900	1.47	0.586	0.160
100	6.41	2.86	1.26	1000	1.38	0.532	0.135

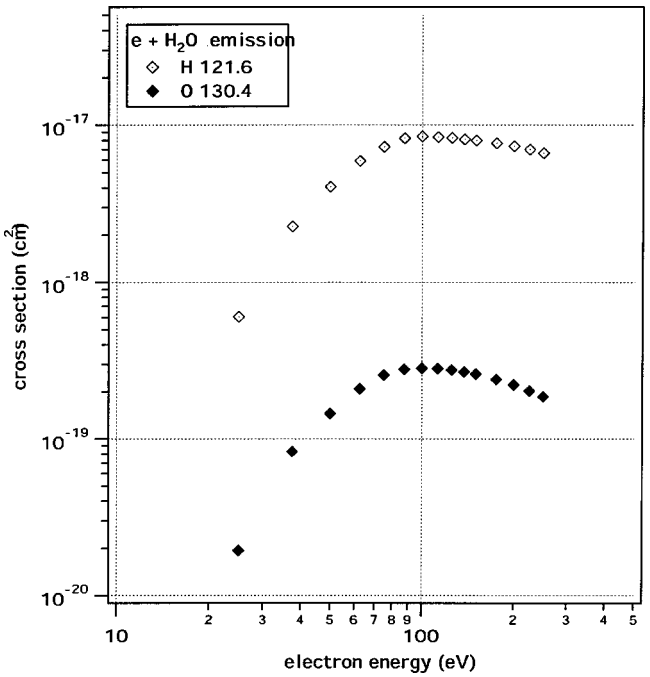

FIG. 17. Cross sections for the emissions of H Lyman α line at 121.6 nm and the O resonance line at 130.4 nm, measured by Morgan and Mentall (Ref. 96). Renormalization of the measured values has been taken as is described in the text.

dence for the Balmer α $(n=3-2)$ line. This is also plotted in Fig 15. Its energy dependence is very similar to that of the Balmer β line, thus confirming the conclusions of Beenakker *et al.* For Balmer lines other than for the transition $n=3-2$, Möhlman and de Heer recorded Q_{emis} at 100 eV. These values are shown in Table 18.

The ratios of those to Q_{emis} for the $n=4-2$ transition are in reasonable agreement with the same ratios obtained by Beenakker *et al.* at 300 eV. Furthermore the absolute value of the Q_{emis} for the Balmer β line measured at 100 eV by Möhlman and de Heer agrees with that of Beenakker *et al.* Müller *et al.*[93] also measured the cross section for the Balmer emissions. Their values at 100 eV are compared in Table 18 with the other two experiments. Considering the experimental uncertainties, the two sets of the cross sections of Möhlman and de Heer and Müller *et al.* are in agreement with each other, except for the Balmer β line. For the Balmer β line, the cross section of Müller *et al.* is a little too small compared with that of Möhlman and de Heer, but agrees with the value of Beenakker *et al.* within their experimental uncertainties.

Table 19 shows the Q_{emis} for the Balmer α (3–2) line measured by Möhlman and de Heer (with an uncertainty of 12%) and Table 20 the Balmer β (4–2) line measured by Beenakker *et al.* (with an uncertainty of 10%).

Emissions from Oxygen Atoms

Beenakker *et al.*[92] obtained the Q_{emis} for the transitions

$$\text{O}\,3p\,^5P-3s\,^5S^o \text{ at } 777.4 \text{ nm},$$

TABLE 21. Emission cross sections for electron impact on H_2O at 200 eV (in 10^{-18} cm^2)

Transition	Morgan[96] (renormalized)	Ajello[97] (renormalized)
H 2–1	7.3 (1.0)[a]	5.6 (0.9)
O 130.4	0.22 (0.03)	0.191 (0.030)

[a]The numbers in the parentheses are the possible errors estimated.

$$\text{O}\,3p\,^3P-3s\,^3S^o \text{ at } 844.7 \text{ nm}.$$

The cross sections for these lines are shown in Fig. 16 and Table 20. Beenakker *et al.* claimed an uncertainty of 20% for both the emissions. The corresponding values at 100 eV are given in Table 18 for comparison with other lines.

Other Emissions

Müller *et al.*[93] observed some other emissions. They obtained the cross sections for

$$\text{OH}^+A\,^3\Pi-X\,^3\Sigma^- \text{ at } 320-420 \text{ nm},$$

$$\text{H}_2\text{O}^+\tilde{A}\,^2A_1-\tilde{X}\,^2B_1 \text{ at } 350-500 \text{ nm}.$$

These cross sections are reported only at 100 eV. Kuchenev and Smirnov[95] measured emissions from $H_2O^+\tilde{A}\,^2A_1-\tilde{X}\,^2B_1$ at 428–763 nm. They report absolute cross section for each rotational line at 50 eV.

10.2. VUV Region

A comprehensive measurement in the VUV region was made by Morgan and Mentall[96] and Ajello.[97] Morgan and Mentall reported the absolute values of Q_{emis} for the energy region from threshold to 300 eV, but only for the hydrogen Lyman α and oxygen resonance lines. Ajello measured the cross section only at 200 eV, but for many lines emitted from the excited states of O, O^+, O^{++}, and H in the region of 40–280 nm. A general review of Q_{emis} in the VUV region was published by van der Burgt *et al.*,[91] and includes a de-

TABLE 22. Cross sections for the emission of H Lyman α (2–1) and O resonance lines produced by electron impact on H_2O, measured by Morgan and Mentall[96] and renormalized

Energy (eV)	Cross section for O 130.4 nm (10^{-19} cm^2)	Cross section for H 121.6 nm (10^{-18} cm^2)
25	0.194	0.601
37.5	0.832	2.27
50	1.45	4.05
62.5	2.09	5.90
75	2.56	7.27
87.5	2.78	8.23
100	2.83	8.45
112.5	2.81	8.39
125	2.75	8.29
137.5	2.68	8.12
150	2.60	7.99
175	2.39	7.64
200	2.22	7.33
225	2.02	6.98
250	1.86	6.65

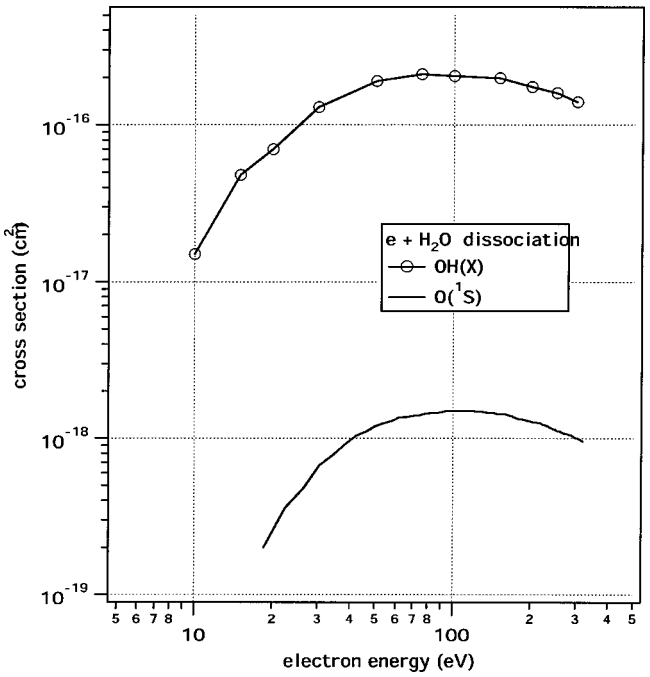

FIG. 18. Cross sections for dissociation of H_2O, for the production of OH (X) (measured by Harb *et al.*, Ref. 101) and O (^1S) (measured by Kedzierski *et al.*, Ref. 100).

tailed discussion of previous experiments. Most of the cross sections in the VUV region are based on relative measurement and resort to some kind of normalization procedure. Van der Burgt *et al.* critically assessed each normalization procedure and proposed, if necessary, renormalization based on more recent and more reliable methods. Ajello normalized his result to the cross section of Lyman α emission from H_2. He used the value (8.18×10^{-18} cm^2 at 100 eV) measured by Shemansky *et al.*[98] Van der Burgt *et al.* determined the best value of this cross section to be 7.3×10^{-18} cm^2. Accordingly Ajello's cross section should be multiplied by 7.3/8.18=0.892. Morgan and Mentall employed in their normalization an average value of the cross sections available for the emission of 130.4 nm line from O_2 (i.e., 3.3×10^{-18} cm^2 at 100 eV). Instead van der Burgt *et al.* recommended using the value (3.05×10^{-18} cm^2) measured by Lawrence[99] and thus the cross section reported by Morgan and Mentall should be multiplied by 3.05/3.3=0.924.

H Lyman α ($2p-1s$) Transition

Figure 17 shows the cross section for the H Lyman α emission at 121.6 nm, measured by Morgan and Mentall and renormalized as above. Table 21 compares the Q_{emis} measured at 200 eV by Morgan and Mentall and by Ajello. Both of the cross sections have been renormalized as above. The agreement of the two cross sections is reasonable, if experimental errors are taken into consideration. The Q_{emis} obtained by Morgan and Mentall (and renormalized) is shown in Table 22. They estimated an error of 13% for these values.

TABLE 23. Cross section for the production of O (^1S) from H_2O by electron impact, measured by Kedzierski *et al.*[100]

Energy (eV)	Cross section (10^{-18} cm^2)	Energy (eV)	Cross section (10^{-18} cm^2)
18.56	0.2	157.16	1.43
22.52	0.36	161.12	1.42
26.48	0.48	165.08	1.40
30.44	0.67	173	1.36
34.4	0.78	176.96	1.34
42.32	1.04	180.92	1.33
50.24	1.20	184.88	1.33
54.2	1.25	192.8	1.30
62.12	1.36	196.76	1.29
70.04	1.39	200.72	1.28
81.92	1.45	212.6	1.26
93.8	1.49	220.52	1.24
101.72	1.50	232.4	1.20
105.68	1.50	240.32	1.16
113.6	1.50	252.2	1.12
121.52	1.49	260.12	1.11
125.48	1.48	272	1.07
133.4	1.47	283.88	1.05
137.36	1.46	291.8	1.03
141.32	1.46	303.68	1.00
145.28	1.45	311.6	0.98
153.2	1.43	319.52	0.95

O Resonance Line

Another intense line in the VUV region is the resonance line of atomic oxygen

$$\text{O}\,2p^3(^4S^o)3s^3S^o-2p^4\,^3P \ \text{ at } \ 130.4 \ \text{nm}.$$

The Q_{emis} measured by Morgan and Mentall (and renormalized as above) is plotted also in Fig. 17. Table 21 gives a comparison of the renormalized values of Morgan and Mentall and Ajello. They agree well with each other. The renormalized Q_{emis} of Morgan and Mentall are given in Table 22 (with an uncertainty of 13%).

Other Emissions

Ajello[97] reported cross sections for many lines emitted from the excited states of O, O^+, O^{++}, and H in the region

TABLE 24. Cross section for the production of OH (X) from H_2O by electron impact, measured by Harb *et al.*[101]

Energy (eV)	Cross section (10^{-16} cm^2)
10	0.15
15	0.48
20	0.7
30	1.3
50	1.9
75	2.1
100	2.05
150	1.98
200	1.75
250	1.6
300	1.4

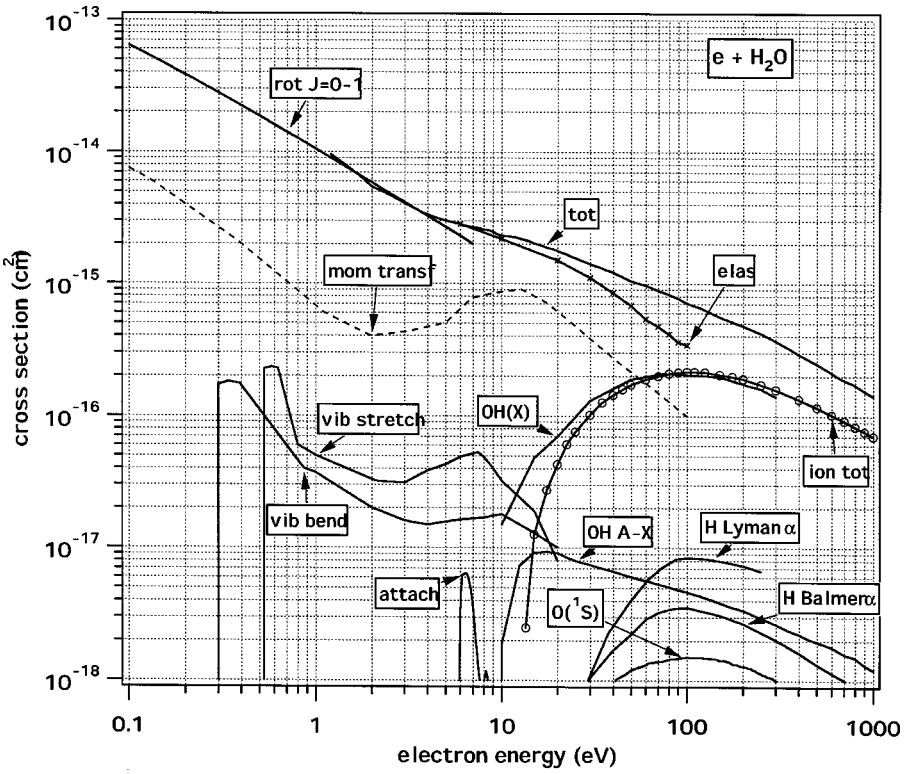

FIG. 19. Summary of the recommended electron collision cross sections for H_2O. Cross sections smaller than 10^{-18} cm^2 are not shown.

of 40–280 nm. The Q_{emis} for those lines were measured at 200 eV. When used, they should be renormalized as stated above. The sum of those cross sections, after being renormalized, is 1.9×10^{-18} cm^2.

11. Dissociation into Neutral, Nonemitting Fragments

When water molecule dissociates upon a collision with electrons, some of the neutral fragments are produced in their ground or metastable states, emitting no radiation (see Table 16). These fragments are difficult to detect but recently new methods have been developed to measure the metastable O (^1S) fragment and the OH in its ground state, $X\,^2\Pi$.

(1) O (^1S)

Kedzierski *et al.*[100] measured the cross section for the production of O (^1S), using a solid xenon matrix detector. The detector is selectively sensitive to O (^1S). The cross section was made absolute using a modified relative flow technique. The signals from H_2O targets were compared with those from CO_2. The cross section for the latter molecule was used as a standard. The resulting cross section is shown in Fig. 18 and Table 23. Kedzierski *et al.*[100] claimed an overall uncertainty of 30% of their data.

(2) OH ($X\,^2\Pi$)

The cross section for the production of the ground state OH was measured by Harb *et al.*[101] They employed a laser-induced-fluorescence technique to detect OH (X). The cross section was made absolute by comparing with the dissociative attachment channel $H_2O\rightarrow OH+H^-$. In so doing, use was made of the attachment cross section determined by Melton[85] (see Sec. 9). The cross section for the production of OH (X) is shown also in Fig. 18. The numerical values are tabulated in Table 24. The final error was estimated to be 36%. Assuming that the excitations of the $1\,^3B_1$ and $1\,^1B_1$ of H_2O yield the fragment OH (X), Gorfinkiel *et al.*[28] compared their theoretical cross scetions for the excitation of those states with the measured values of dissociation cross section for OH (X). It was found that the theoretical cross section was too large at the energies below 10 eV and became close to the dissociation cross section at around 15 eV (the highest energy for which the calculation was done). This discrepancy may be due to the limitation of the calculation, i.e., the one-dimensional model of nuclear motion. More flexibility of nuclear motion would open other channels, reducing the theoretical probability of the excitation of the relevant states.

Since there remains a possibility that the dissociative attachment cross section values of Melton may contain a systematic error, it is important to remeasure the attachment cross section and use these new values to renormalize the OH ($X\,^2\Pi$) cross section.

12. Summary and Future Problems

Figure 19 provides a summary of the present compilation of cross sections for $e+H_2O$ collisions. Cross sections tabulated for the following processes are shown in the figure: total scattering (Table 3), elastic scattering (Table 4), momentum transfer (Table 5), rotational transition $J=0\rightarrow1$

(Table 8), vibrational excitation (Table 9), total ionization (Table 11), electron attachment to produce H^- (Table 13), emissions of OH ($A-X$) (Table 17), H Lyman α (Table 22), and H Balmer α (Table 19), and productions of O(^1S) (Table 23) and OH(X) (Table 24). Cross sections recommended for other processes are smaller than 10^{-18} cm^2 and so are not shown in this figure.

To make the cross section data set more comprehensive and more accurate, we need further experimental studies, particularly in the following areas:

(1) A measurement of total scattering cross section is needed at low energies particularly below 1 eV, with care taken to allow for any necessary forward-scattering corrections.
(2) Elastic scattering cross sections in the energy region below 4 eV are need to be measured using the magnetic angle changing technique. Especially the forward scattering peak predicted by theory should be studied experimentally.
(3) No beam–beam experiments provide information on the rotational cross sections for individual transition. A careful analysis of the profile of the elastic peak in the energy loss spectra could provide the information of the rotational cross section.
(4) More elaborate and quantitatively detailed measurements of the vibrational cross sections would be desirable in the energy range: (a) around 7.5 eV and (b) near threshold (below 1 eV). The presence of a resonant process in the former region must be explored.
(5) The last measurement of the absolute values of dissociative attachment cross section was more than 30 years ago and may contain kinetic energy discrimination effects. It therefore should be repeated.
(6) A detection of neutral dissociation fragments is of prime importance, since there is currently no information of the production of O(^3P) and O(^1D) fragments.
(7) No beam experiment has been done to obtain absolute cross section for the excitation of electronic states. Since the energy loss spectra have been measured several times, it is, in principle, possible to experimentally derive DCS for the electronic excitation from the spectra. Most of the excitations are expected to lead to dissociation of the molecule, but it would be of great interest to reveal the details of the dissociation path ways from each electronic state.
(8) The cross sections dealt with in the preceding sections can depend on the internal energy of the molecule and hence on the gas temperature. In the present paper, however, experimental data are collected from the measurement at room temperature. Any study of the dependence of the cross section on the gas temperature may be useful for applications.

Once electron interactions with water in the gas phase have been established, the influence of phase should be considered. As is indicated in the Introduction (Sec. 1), water is the most important biological molecule. Electron interactions with a water molecule are the fundamental processes in the radiation action on biological matter. However in biology, water is in liquid phase. Due to the scarcity of experimental and theoretical knowledge of the electron interaction with liquid water, the gaseous water is often used to simulate the biological medium. This is a challenging problem and it is necessary to find if and how cross sections in the gas phase can be modified to estimate cross sections in liquid phase which will be used to estimate radiation effects in biological systems.

13. Acknowledgments

During the course of the present work, many colleagues provided the authors with valuable information about the data considered here. Particular thanks are due to Jonathan Tennyson, who gave them detailed results of the calculation of his group. Discussion with him was helpful in the evaluation of the cross section data. They are also indebted to Hyuck Cho, Mohammed Yousfi, and Bill McConkey for sending them numerical data of the cross section they obtained. They also thank the EC EPIC Network (Contract No. RTN-0153) for support.

14. References

[1] For the spectroscopic observation of water, see P. F. Bernath, Phys. Chem. Chem. Phys. **4**, 1501 (2002).
[2] B. Nisini, Science **290**, 1513 (2000).
[3] F. W. Taylor, Rep. Prog. Phys. **65**, 1 (2002).
[4] X. Xie and M. J. Mumma, Astrophys. J. **386**, 720 (1992).
[5] For example, M. A. Tas, E. M. van Veldhuizen, and W. R. Rutgers, J. Phys. D **30**, 1636 (1997).
[6] S. Uehara, H. Nikjoo, and D. T. Goodhead, Rad. Res. **152**, 202 (1999).
[7] IAEA-TECDOC-799, *Atomic and Molecular Data for Radiotherapy and Radiation Research* (International Atomic Energy Agency, 1995).
[8] G. P. Karwasz, R. S. Brusa, and A. Zecca, Rivista Nuovo Cimento **24**, No. 1 (2001).
[9] T. Shirai, T. Tabata, and H. Tawara, Atomic Data Nucl. Data Tables **79**, 143 (2001).
[10] M. Hayashi, *Bibliography of Electron and Photon Cross Sections with Atoms and Molecules*, in *20th Century–Water Vapour*–NIFS-Data-81 (National Institute for Fusion Science, Oroshi-cho, Toki, Japan, 2003).
[11] Y. Itikawa, editor, *Photon and Electron Interactions with Atoms, Molecules and Ions*, Landolt-Börnstein, Volume I/17, Subvolume C (Springer, New York, 2003).
[12] K. Kuchitsu, editor, *Structure Data of Free Polyatomic Molecules*, Landolt-Börnstein, Volume II/25, Subvolume A Inorganic Molecules (Springer, New York, 1998), p. 296.
[13] S. G. Lias, ''Ionization Energy Evaluation'' in *NIST Chemistry WebBook*, NIST Standard Reference Database Number 69, edited by P. J. Linstrom and W. G. Mallard (National Institute of Standards and Technology, Gaithersburg, MD, 2001) ⟨http://webbook.nist.gov⟩.
[14] B. Ruscic *et al.*, J. Phys. Chem. A **106**, 2727 (2002).
[15] J. D. Demaison, A. Dubralle, W. Hüttner, and E. Tiermann, *Molecular Constants, Mostly from Microwave, Molecular Beam, and Electron Resonance Spectroscopy*, Landolt-Börnstein, Volume II/14 subvolume a (Springer, New York, 1982), p. 602.
[16] T. R. Dyke and J. S. Muenter, J. Chem. Phys. **59**, 3125 (1973).
[17] J. Verhoeven and A. Dymanus, J. Chem. Phys. **52**, 3222 (1970).
[18] W. F. Murphy, J. Chem. Phys. **67**, 5877 (1977).
[19] T. Shimanouchi, *Tables of Molecular Vibrational Frequencies Consolidated Volume I*, NBS Ref. Data Series 39 (U.S. Government Printing Office, Washington D.C., 1972).

[20] O. L. Polyansky, P. Jensen, and J. Tennyson, J. Chem. Phys. **105**, 6490 (1996).
[21] C. Szmytkowski, Chem. Phys. Lett. **136**, 363 (1987).
[22] A. Zecca, G. Karwasz, S. Oss, R. Grisenti, and R. S. Brusa, J. Phys. B **20**, L133 (1987).
[23] H. Nishimura and K. Yano, J. Phys. Soc. Jpn. **57**, 1951 (1988).
[24] Z. Saglam and N. Aktekin, J. Phys. B **23**, 1529 (1990).
[25] Z. Saglam and N. Aktekin, J. Phys. B **24**, 3491 (1991).
[26] M. Kimura, O. Sueoka, A. Hamada, and Y. Itikawa, Adv. Chem. Phys. **111**, 537 (2000).
[27] O. Sueoka, S. Mori, and Y. Katayama, J. Phys. B **19**, L373 (1986).
[28] J. D. Gorfinkiel, L. A. Morgan, and J. Tennyson, J. Phys. B **35**, 543 (2002).
[29] A. Hamada and O. Sueoka, J. Phys. B **27**, 5055 (1994).
[30] Y. Okamoto, K. Onda, and Y. Itikawa, J. Phys. B **26**, 745 (1993).
[31] C. Szmytkowski, K. Maciag, P. Koenig, A. Zecca, S. Oss, and R. Grisenti, Chem. Phys. Lett. **179**, 114 (1991).
[32] A. Danjo and H. Nishimura, J. Phys. Soc. Jpn. **54**, 1224 (1985).
[33] A. Katase, K. Ishibashi, Y. Matsumoto, T. Sakae, S. Maezono, E. Murakami, K. Watanabe, and H. Maki, J. Phys. B **19**, 2715 (1986).
[34] T. W. Shyn and S. Y. Cho, Phys. Rev. A **36**, 5138 (1987).
[35] W. M. Johnstone and W. R. Newell, J. Phys. B **24**, 3633 (1991).
[36] T. W. Shyn and A. Grafe, Phys. Rev. A **46**, 4406 (1992).
[37] S. J. Buckman, M. J. Brunger, and M. T. Elford, in *Photon and Electron Interactions with Atoms, Molecules and Ions*, Landolt-Börnstein Vol. I/17, Subvolume C, edited by Y. Itikawa (Springer, New York, 2003).
[38] H. Cho, Y. S. Park, H. Tanaka, and S. J. Buckman, J. Phys. B **37**, 625 (2004).
[39] A. Faure, J. D. Gorfinkiel, and J. Tennyson, Mon. Not. R. Astron. Soc. **347**, 323 (2004).
[40] M. Yousfi and M. D. Benabdessadok, J. Appl. Phys. **80**, 6619 (1996).
[41] J. Tennyson, N. F. Zobov, R. Williamson, O. L. Polyansky, and P. F. Bernath, J. Phys. Chem. Ref. Data **30**, 735 (2001).
[42] A. Faure, J. D. Gorfinkiel, and J. Tennyson, J. Phys. B **37**, 801 (2004).
[43] F. A. Gianturco, S. Meloni, P. Paioletti, R. R. Lucchese, and N. Sanna, J. Chem. Phys. **108**, 4002 (1998).
[44] K. Jung, T. Antoni, R. Müller, K.-H. Kochem, and H. Ehrhardt, J. Phys. B **15**, 3535 (1982).
[45] G. Seng and F. Linder, J. Phys. B **9**, 2539 (1976).
[46] T. W. Shyn, S. Y. Cho, and T. E. Cravens, Phys. Rev. A **38**, 678 (1988).
[47] A. El-Zein, M. J. Brunger, and W. R. Newell, J. Phys. B **33**, 5033 (2000).
[48] A. El-Zein, M. J. Brunger, and W. R. Newell, Chem. Phys. Lett. **319**, 701 (2000).
[49] M. J. Brunger, S. J. Buckman, and M. T. Elford, in *Photon and Electron Interactions with Atoms, Molecules and Ions*, Landolt-Börnstein Vol. I/17, Subvolume C, edited by Y. Itikawa (Springer, New York, 2003).
[50] A. Jain and D. G. Thompson, J. Phys. B **16**, L347 (1983).
[51] T. Nishimura and Y. Itikawa, J. Phys. B **28**, 1995 (1995).
[52] O. Moreira, D. G. Thompson, and B. M. McLaughlin, J. Phys. B **34**, 3737 (2001).
[53] K. Rohr, J. Phys. B **10**, L735 (1977).
[54] T. Nishimura and F. A. Gianturco, Europhys. Lett. **65**, 179 (2004).
[55] M. Allan and O. Moreira, J. Phys. B **35**, L37 (2002).
[56] M. Ben Arfa, F. Edard, and M. Tronc, Chem. Phys. Lett. **167**, 602 (1990).
[57] W. F. Chan, G. Cooper, and C. E. Brion, Chem. Phys. **178**, 387 (1993).
[58] P. Gürtler, V. Saile, and E. E. Koch, Chem. Phys. Lett. **51**, 386 (1977).
[59] A. Chutjian, R. I. Hall, and S. Trajmar, J. Chem. Phys. **63**, 892 (1975).
[60] W. A. Goddard III and W. J. Hunt, Chem. Phys. Lett. **24**, 464 (1974).
[61] N. W. Winter, W. A. Goddard III, and F. W. Bobrowicz, J. Chem. Phys. **62**, 4325 (1975).
[62] R. van Harrevelt and M. C. van Hemert, J. Chem. Phys. **112**, 5777 (2000).
[63] J. J. Olivero, R. W. Stagat, and A. E. S. Green, J. Geophys. Res. **77**, 4797 (1972).
[64] M. Zaider, D. J. Brenner, and W. E. Wilson, Rad. Res. **95**, 231 (1983).
[65] D. A. Edmonson, J. S. Lee, and J. P. Doering, J. Chem. Phys. **69**, 1445 (1978).
[66] D. Cvejanovic, L. Andric, and R. I. Hall, J. Phys. B **26**, 2899 (1993).
[67] H. P. Pritchard, V. McKoy, and M. A. P. Lima, Phys. Rev. A **41**, 546 (1990).
[68] T. J. Gil, T. N. Rescigno, C. W. McCurdy, and B. H. Lengsfield III, Phys. Rev. A **49**, 2642 (1994).
[69] M.-T. Lee, S. E. Michelin, T. Kroin, L. E. Machado, and L. M. Brescansin, J. Phys. B **28**, 1859 (1995).
[70] L. A. Morgan, J. Phys. B **31**, 5003 (1998).
[71] S. Trajmar, W. Williams, and A. Kuppermann, J. Chem. Phys. **58**, 2521 (1973).
[72] E. N. Lassettre and E. R. White, J. Chem. Phys. **60**, 2460 (1974).
[73] K. N. Klump and E. N. Lassettre, Can. J. Phys. **53**, 1825 (1975).
[74] B. G. Lindsay and M. A. Mangan, in *Photon and Electron Interactions with Atoms, Molecules and Ions*, Landolt-Börnstein Vol. I/17, Subvolume C, edited by Y. Itikawa (Springer, New York, 2003).
[75] H. C. Straub, B. G. Lindsay, K. A. Smith, and R. F. Stebbings, J. Chem. Phys. **108**, 109 (1998).
[76] M. V. V. S. Rao, I. Iga, and S. K. Srivastava, J. Geophys. Res. **100**, 26421 (1995).
[77] J. Schutten, F. J. de Heer, H. R. Moustafa, A. J. H. Boerboom, and J. Kistemaker, J. Chem. Phys. **44**, 3924 (1966).
[78] W. Hwang, Y.-K. Kim, and M. E. Rudd, J. Chem. Phys. **104**, 2956 (1996).
[79] D. Lefaivre and P. Marmet, Can. J. Phys. **56**, 1549 (1978).
[80] H. Ehrhardt and A. Kresling, Z. Naturforschg. **22a**, 2036 (1967).
[81] M. A. Bolorizadeh and M. E. Rudd, Phys. Rev. A **33**, 882 (1986).
[82] C. Champion, J. Hanssen, and P. A. Hervieux, J. Chem. Phys. **117**, 197 (2002).
[83] V. Tarnovsky, H. Deutsch, and K. Becker, J. Chem. Phys. **109**, 932 (1998).
[84] Y. Itikawa, in *Photon and Electron Interactions with Atoms, Molecules and Ions*, Landolt-Börnstein Vol. I/17, Subvolume C, edited by Y. Itikawa (Springer, New York, 2003).
[85] C. E. Melton, J. Chem. Phys. **57**, 4218 (1972).
[86] R. N. Compton and L. G. Christophorou, Phys. Rev. **154**, 110 (1967).
[87] D. S. Belic, M. Landau, and R. I. Hall, J. Phys. B **14**, 175 (1981).
[88] M. Jungen, J. Vogt, and V. Staemmler, Chem. Phys. **37**, 49 (1979).
[89] K. Becker, B. Stumpf, and G. Schulz, Chem. Phys. **53**, 31 (1980).
[90] D. A. Vroom and F. J. de Heer, J. Chem. Phys. **50**, 1883 (1969).
[91] P. J. M. van der Burgt, W. B. Westerveld, and J. S. Risley, J. Phys. Chem. Ref. Data **18**, 1757 (1989).
[92] C. I. M. Beenakker, F. J. de Heer, H. B. Krop, and G. R. Möhlmann, Chem. Phys. **6**, 445 (1974).
[93] U. Müller, Th. Bubel, and G. Schulz, Z. Phys. D **25**, 167 (1993).
[94] G. R. Möhlmann and F. J. de Heer, Chem. Phys. **40**, 157 (1979).
[95] A. N. Kuchenev and Yu. M. Smirnov, Can. J. Phys. **74**, 267 (1996).
[96] H. D. Morgan and J. E. Mentall, J. Chem. Phys. **60**, 4734 (1974).
[97] J. M. Ajello, Geophys. Res. Lett. **11**, 1195 (1984).
[98] D. E. Shemansky, J. M. Ajello, and D. T. Hall, Astrophys. J. **296**, 765 (1985).
[99] G. M. Lawrence, Phys. Rev. A **2**, 397 (1970).
[100] W. Kedzierski, J. Derbyshire, C. Malone, and J. W. McConkey, J. Phys. B **31**, 5361 (1998).
[101] T. Harb, W. Kedzierski, and J. W. McConkey, J. Chem. Phys. **115**, 5507 (2001).